Recent Developments in the Fabrication and Operation of Germanium Detectors

Kai Vetter*

Glenn T. Seaborg Institute, Lawrence Livermore National Laboratory, Livermore, California 94550; email: kvetter@llnl.gov

Annu. Rev. Nucl. Part. Sci. 2007. 57:363–404

First published online as a Review in Advance on June 28, 2007

The *Annual Review of Nuclear and Particle Science* is online at http://nucl.annualreviews.org

This article's doi:
10.1146/annurev.nucl.56.080805.140525

0163-8998/07/1123-0363$20.00

Key Words

Ge detectors, Ge detector technologies, gamma-ray tracking, Compton imaging, neutrinoless double-beta decay

Abstract

Although developed and first demonstrated more than 40 years ago, germanium detectors still represent the gold standard in detecting γ radiation for energies ranging from approximately 100 keV to 10 MeV. The combination of high-efficiency and excellent energy resolution and many recent technological developments have significantly increased the range of applications for Ge detectors. We review the state of the art in the fabrication and operation of Ge detectors by mapping recent developments in Ge detector technologies to a range of applications. These include research in nuclear physics, fundamental physics, and astrophysics, as well as applications in medical imaging and homeland security. Ge detector technologies will remain vitally important for applied and basic research instruments for high-sensitivity γ-ray detection in the future.

Contents

1. INTRODUCTION

Despite the persistent perception of germanium detectors as being outlived by other detectors for many years now, and despite significant investments in alternative detector materials and concepts, the range of applications and variety of implementations for Ge detectors have been and are still expanding. This is on the one hand due to technological advances in Ge detector and related technologies, which enable the realization of new and improved detection concepts, and on the other hand due to experimental and operational requirements, which are driving the technological advances.

Since A.J. Tavendale's review in 1967 on *Semiconductor Nuclear Radiation Detectors*, no paper has addressed the enormous advances that have been achieved in Ge detector and related technologies in this series (1). Review papers associated with the advances in Ge detector technologies were published in the 1980s and 1990s and focused on the study of specific features in nuclei (2–4). At the time of the Tavendale paper, the use of Ge detectors or silicon detectors for γ-ray detection was still in its infancy. Tavendale reports on the first lithium-drifted coaxial Ge detectors with volumes of 23 ml with, at that time, excellent energy resolution of 5.6 keV at an energy of 1368 keV. Considerable, almost inconceivable, progress in the manufacturing of large-volume detectors and processing electronics since then is the reason that, more than 40 years after the introduction of Ge as a feasible γ-ray detector material, it still provides unchallenged performance in terms of efficiency and energy resolution. Ge detectors have been built with volumes larger than 800 ml (5) and an energy resolution of 0.2 keV at low energies, which is close to the statistical limit (6). These outstanding properties are due to the unique combination of a small band gap of the elemental semiconductor Ge, very large electron and hole mobilities and lifetimes, and the fact that large crystal sizes with the highest purity and a minimum of crystal defects can

be grown. The development of low-noise electronics was critical as well to achieving the high-energy resolution, particularly at low energies.

In addition to advances in the growth and purification techniques, which enable the fabrication of large-volume detectors, improved contact segmentation technologies provide the basis to measure positions and energies of individual γ-ray interactions with high accuracy and efficiency. This capability is now being used to determine the path of the γ-ray in the detector, which has a profound impact for many applications. It allows construction of arrays based on a closed shell of more than 100 of these detectors for nuclear physics experiments, providing unprecedented sensitivity in detecting many γ-rays simultaneously. In addition, the combination of high efficiency and granularity provided by segmented Ge detectors allows us to build efficient Compton-scattering-based γ-ray imaging systems, so-called Compton cameras. Compton cameras can image γ-ray sources without using heavy collimators over a large field of view, finding applications in astrophysics, biomedical imaging, nuclear nonproliferation and safeguards, and homeland security.

Complementary to the developments in Ge detector technologies themselves, advances in electronics that provide low-noise signal amplification and filtering and fast digitization were essential to realizing their demonstrated capabilities. Advances in Ge detector technologies were accompanied by advances in electronics, originally in analog signal processing primarily and more recently in digital signal processing. Digital signal processing provides higher count rate capabilities and compensation for ballistic deficit effects, two features difficult to address with analog processing. They provide more flexibility in adapting different detectors and detector configurations and in the implementation of more complex filters (e.g., adaptive and time dependent). Only the combination of two-dimensional segmentation and the digitization with high sampling rates and high resolution enabled the precise analysis of pulse shapes in Ge detectors, providing the three-dimensional position and energies in large-volume Ge detectors. Pulse-shape analysis is now employed to determine positions and energies of interactions, to distinguish between γ-rays that deposited only a fraction of the full energy, and to distinguish between γ-rays and, for example, electrons interacting in the detector by distinguishing between single and multiple interactions. On the one hand, this distinction allows the suppression of electron or beta background, for example, in astrophysics applications aimed at measuring γ-rays. On the other hand, it allows suppression of γ-rays for fundamental physics applications such as the search for the neutrinoless double-beta ($0\nu\beta\beta$) decay in isotopically enriched ^{76}Ge detectors (7).

The majority of applications for Ge detectors still relies on the γ-ray detection by measuring the ionization of Ge atoms. However, over the past 20 years, significant progress was made in measuring the heat generated by particles or photons, which allows a much improved energy resolution and sensitivities to smaller energy depositions. Ge detectors can be operated as bolometers at sub-Kelvin temperatures, measuring the number of phonons by observing the temperature rise in very low heat capacity thermistors. Although not necessarily implemented with Ge, this method provides the possibility of measuring the ionization and the heat simultaneously, which allows the discrimination, for example, of neutral particles and γ-rays.

In addition to using Ge as a particle or photon absorber, heavily doped Ge, such as neutron-transmutation-doped (NTD) Ge, is also being used as a very sensitive thermometer or thermistor owing to its very small and uniform heat capacity (8).

In the following we provide a brief historical review starting from the first demonstration of a Li-drifted Ge [Ge(Li)] detector in the 1960s to the most recent developments in large Ge detector arrays. A technical review briefly discusses some basic principles in the operation of Ge detectors. In Section 3 we discuss recent technical advances. Section 4 presents applications that drove or benefited from these advances. In Section 5 we attempt a brief outlook to the future of Ge detector and related technologies and conclude with a brief summary in Section 6. The aim of this review is not to be complete and encyclopedic but rather exemplary—to provide an overview on the breadth of developments of the recent past.

1.1. Historical Review

Since the first demonstration in the early 1960s, Ge detectors have undergone a remarkable development and now represent one of the detectors of choice for γ-ray detection. Although single crystals of Ge were grown already in 1950 (9), the first practicable Ge detector material was produced in 1960 using Li-donor compensation of p-type crystals (10, 11). These Ge(Li) detectors opened the field of high-resolution γ-ray spectroscopy. The Li drifting process was required to compensate for the remaining acceptor impurities in the Ge material, which allowed the fabrication of Ge detectors with sensitive volumes of up to 100 ml.

Owing to the much improved energy resolution as compared with NaI(Tl) detectors, Ge(Li) detectors became the state of the art for γ-ray spectroscopy in the 1960s and 1970s to study the structure of atomic nuclei. By 1970, arrangements of two or more of these detectors were used to measure coincidence relationships between γ-rays emitted from the nucleus in order to construct detailed level schemes of the excited states.

The drawback of Ge(Li) detectors is the high mobility of interstitial Li donors in Ge, which requires the detector temperature to be kept close to 77 K to prevent the Li from diffusing out of the detector, thereby removing the compensation of the acceptor impurity and making the detector inoperable, and requiring a redrifting process. The cooling requirement is a drawback not only when operating, storing, or transporting detectors, but also during the fabrication process and when transferring the detector between cryostats. In addition, the Li drifting process takes several weeks and limits the maximum size of the Ge detector. Finally, Li drifting can be performed only in p-type material, which is significantly more susceptible to radiation damage in coaxial detectors, which represent the majority of used Ge detectors. The repair of radiation damage by thermal annealing is almost impossible for Li-drifted materials.

In 1971, Hall (12) proposed the possibility of purifying and growing Ge of the high purity required without the need for subsequent Li drifting. It took approximately 10 more years before high-purity germanium (HPGe) detectors could be produced, in part owing to the seminal work by Hall at General Electric and Hansen & Haller at Lawrence Berkeley National Laboratory (13, 14). Around 1980, Ge(Li) detectors

were replaced by HPGe detectors. Since then, the crystal growth process was further refined, which increased the maximum achievable diameter from approximately 60 mm in the 1980s to almost 100 mm today. P-type detectors with a diameter of 98 mm, a length of 110 mm, a corresponding volume of 830 ml, and a weight of 4.4 kg have been built (5). N-type detectors with diameters of 7 cm and lengths of 14 cm have been built for the Versatile and Efficient Gamma detector (VEGA). As a matter of fact, four of these large-volume detectors are mounted in one cryostat in a clover-like arrangement, which, by summing γ-rays from all detectors, can be treated as one large $14 \times 14 \times 14$ cm^3 or 2.5 liter Ge detector with a weight of 12 kg (15).

To improve the spectral response of Ge detectors, so-called anti-Compton shields were introduced in the 1980s. These shields are made of high-density scintillating detectors that surround the Ge detector to suppress events in which only part of the energy is deposited in the Ge. In this way, the continuous Compton background can be reduced and the overall peak-to-background ratio increased significantly. By 1985, small arrays of up to 12 Compton-suppressed Ge detectors were being widely used for nuclear physics experiments (16). The culmination of these types of arrays is Gammasphere in the United States (17) and Euroball in Europe (18). **Figure 1** shows the evolution of γ-ray detector systems in terms of the so-called resolving power. The resolving power is defined as the inverse of the sensitivity or observational limit, for example, indicating the weakest γ-ray decay channel, which can be resolved in an experiment. In addition, the figure illustrates the gain in sensitivity to measure higher spin states populated with lower intensity in the ground state rotational band and the extracted moment of inertia observed with different devices in ^{156}Dy. While the relative intensity reflects the increase of the resolving power, the moment-of-inertia plot reveals new physics associated with increased angular momentum of the nucleus (e.g., it reflects the alignments of neutron and proton angular momentum along the axis of rotation owing to Coriolis effects, the loss of suprafluid correlations and band termination, and the associated loss of quantum collectivity). Remarkably, in the ^{156}Dy case, almost every significant increase in detection sensitivity was associated with the discovery of a new phenomenon.

The current state-of-the-art detector arrays, such as Gammasphere (shown in **Figure 2**) or Euroball, comprise approximately 100 or more Compton-suppressed Ge detectors. These systems, which were built in the 1990s, have an absolute efficiency of approximately 10% for detecting the full energy of a 1-MeV γ-ray and a peak-to-total ratio of approximately 55%. Both efforts introduced technologies critical for the next-generation γ-ray spectrometer currently being built, the γ-ray-tracking-based instruments. Gammasphere introduced segmented coaxial detectors into nuclear physics applications to reduce the degradation of the intrinsic energy resolution due to Doppler broadening in in-beam experiments. Euroball introduced cryostats with seven large-volume Ge detectors—so-called cluster detectors—with each detector mounted in a hermetically sealed vacuum capsule. Mounting several detectors in one cryostat increases the efficiency and improves the peak-to-background ratio by adding the energies of all detectors within one cryostat; the encapsulation ensures the reliable operation and potentially necessary annealing procedures. In parallel to the development of large arrays of Ge detectors and

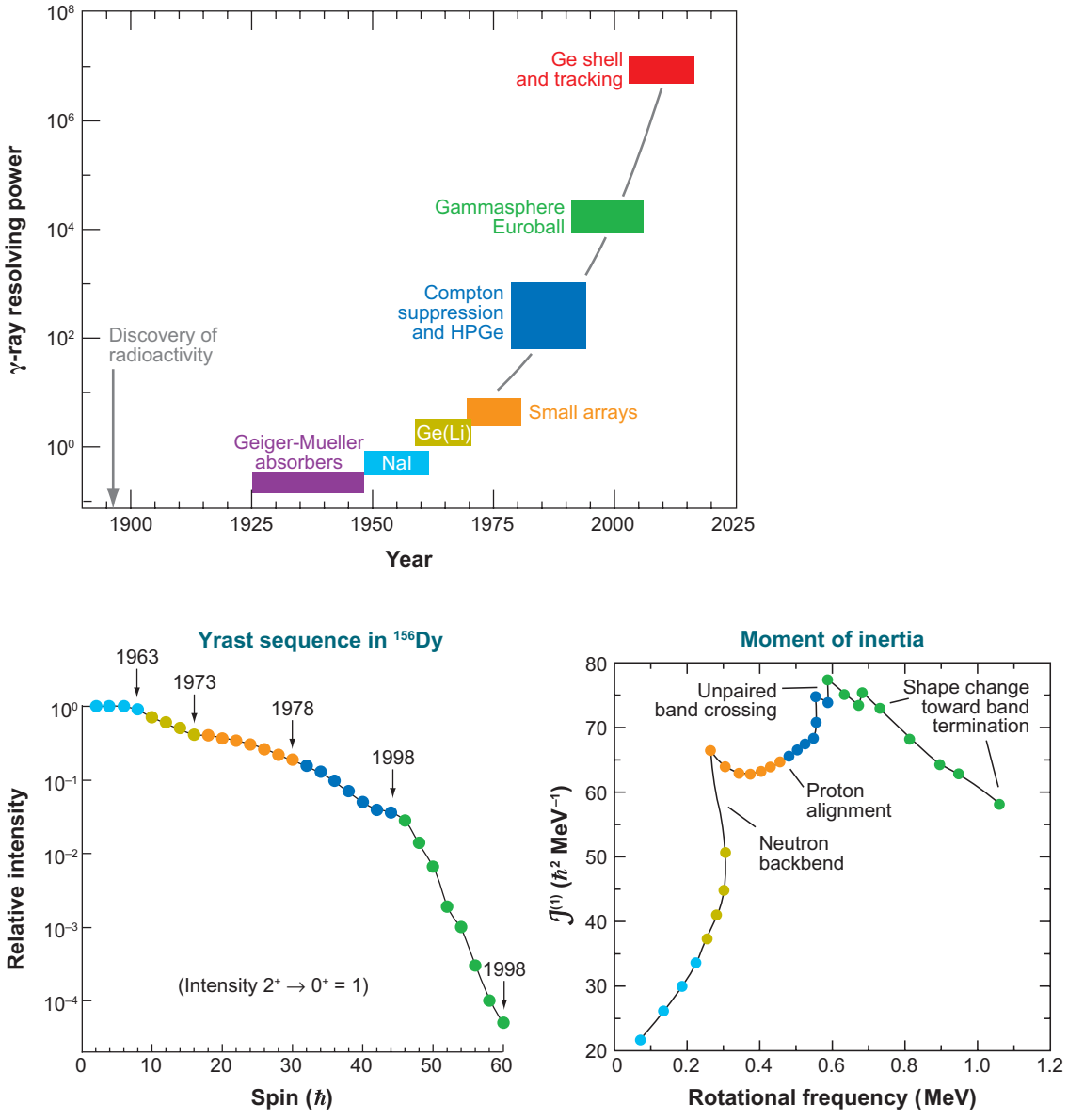

Figure 1

The evolution of γ-ray detectors in terms of resolving power. The lower left panel shows the corresponding observational limit as relative intensity measured in ^{156}Dy as a function of spin. The lower right panel shows the associated moment of inertia as a function of rotational frequency. HPGe, high-purity germanium; $\mathcal{J}^{(1)}$, moment of inertia.

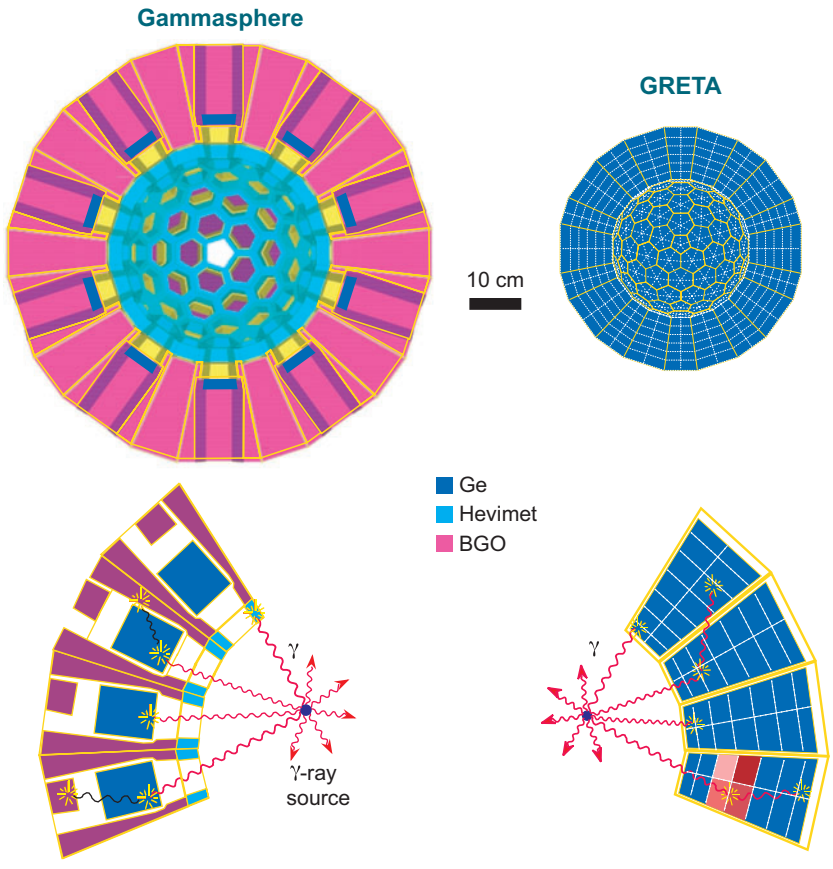

Figure 2

Comparison between the current state-of-the-art detector Gammasphere (*left*) and the proposed Gamma-Ray Energy Tracking Array (GRETA) (*right*). Proposed γ-ray tracking arrays such as GRETA consist only of Ge detectors; Compton shields, for example, made of bismuth germanate (BGO), and absorbers are removed. The lower panels indicate the two different approaches. While anti-Compton shields suppress cross-scattering between Ge crystals and the hevimet absorber prevents direct hits of the shields to prevent false suppression, a γ-ray tracking array accepts all γ-rays, significantly increasing the efficiency.

reflecting a significant worldwide effort to study atomic nuclei far away from the valley of stability at new radioactive facilities, smaller and more compact arrays have been built or are currently being built. Examples of such arrays are Exogam at the Grand Accélérateur National d'Ions Lourdes (GANIL) facility in France (19, 20), Miniball at CERN in Switzerland (21–23), the Segmented Germanium Array (SeGA) at Michigan State University (24), and most recently the TRIUMF-ISAC Gamma-Ray Escape Suppressed Spectrometer (TIGRESS) at TRIUMF in Canada (25).

Although both types of arrays, Gammasphere-like primarily for stable beam facilities and Exogam-like with the focus on radioactive beam facilities, represent a large increase in efficiency and resolving power in contrast to previous arrays, they are ultimately limited by the anti-Compton suppressor shields and the limited efficiency of individual Ge detector systems. The removal of the Compton suppressor would allow the solid angle coverage to increase by roughly a factor of two and, in addition, would enable adding energies of several detectors, increasing the efficiency, for example, for the detection of a 1.3-MeV γ-ray by another factor of two. Ultimately, the efficiency for detecting the full energy of 1.3 MeV for a closed shell built purely with Ge detectors is approximately 60%, limited only by the finite size of the Ge crystals,

gaps, and absorption in mounting structures. However, the inability to distinguish between two γ-rays emitted and detected simultaneously and one γ-ray interacting with two detectors prevented the introduction of pure Ge shells for nuclear physics experiments. To separate multiple and simultaneous γ-rays sufficiently, more than 1000 detectors would be required, which is prohibitive owing to cost. The solution is to track the interactions of all γ-rays to identify and separate the emitted γ-rays even if several interact in one detector, as shown in **Figure 2**. Owing to the advances over the past 10 years in two-dimensional segmentation of large-volume Ge detectors and in digital signal processing, it is now possible to build detectors that can track γ-rays by measuring energies and positions of individual γ-ray interactions with high efficiency and accuracy.

The concept of γ-ray tracking in large two-dimensional segmented Ge detectors allows us to significantly increase the sensitivity in most nuclear physics experiments, ranging from radioactive beam experiments with the most exotic and rare nuclei to stable beam facilities to probe the nuclear structure at the highest attainable spins associated with the largest number of γ-rays and most complex decay schemes. In addition, it also enables us to determine the incident direction of γ-rays without using a collimator. Because it uses the Compton scattering formula to correlate the measured energies and positions with the incident angle, these systems are called Compton cameras. Because γ-rays, particularly at energies above 100 keV, cannot be focused easily, γ-ray imaging systems normally use collimator or aperture systems to project a source-location-specific pattern on a γ-ray detector. Examples are Anger cameras, consisting typically of a parallel-hole collimator in front of a position-sensitive NaI(Tl) detector, or coded-aperture or rotation-modulation systems (26–28). The latter two project the object by modulating the intensity spatially or temporarily, respectively. The drawback of the collimator-based approach is the heavy collimator, which is required to generate a source-location-specific pattern on the detector. It not only makes the system heavy, particularly for higher γ-ray energies, it also introduces artifacts owing to scattering in the collimator and penetration of the collimator. Furthermore, it requires the γ-rays to enter through the collimator, limiting the solid angle that can be imaged—the so-called field of view—and, for many applications, requires heavy shielding all around the detector to reduce the background. Tracking has the additional benefits of increasing the overall sensitivity by correlating the image and the track information. In γ-ray imaging, the improvement due to γ-ray tracking is currently being explored in many areas, ranging from biomedical research (29, 30) to homeland security (31, 32) to astrophysics (33, 34). It is even being discussed for nuclear physics experiments with radioactive beams that distinguish between γ-rays of interest from the target and γ-rays from the radioactive-beam-related background. For these applications, Ge detectors provide high sensitivity owing to the high-energy and position resolution in combination with the high efficiency that can be achieved with large-volume detectors. The full γ-ray or event reconstruction associated with γ-ray tracking is also currently evaluated for fundamental physics experiments such as Majorana, which aims at observing the $0\nu\beta\beta$ decay in enriched ^{76}Ge detectors. Here, a partial or a full γ-ray reconstruction provides additional information to distinguish between the beta-decay signal and predominantly γ-ray background (7). Although

these efforts are driving to a large part the developments in Ge-detector-related technologies, Ge detectors are now widely used in many other applications such as nuclear emergency response; nuclear counting facilities; safeguards applications; secondary inspection, for example, at borders or port of entries; or airborne surveillance, for example, for mining or other geological purposes. Many of these systems are now very compact, either with small liquid nitrogen dewars or operating cryogen-free by mechanically cooling the detectors and read out with fast-sampling analog-to-digital converters, where signal processing and filtering are performed digitally.

Complementary to these efforts, Ge detectors working as thermometers have been developed and are operating at much lower temperatures, for example, milli-Kelvin, providing the ability to simultaneously measure both the heat dissipation through the generations of vibrations or phonons and the ionization. The type of recoil can be identified because the ionization signal of a nuclear recoil is quenched as compared with an electron recoil. Also, because nuclear recoils are generated by heavier particles such as neutrons or potentially weakly interacting massive particles (WIMPs) and electron recoils are generated predominantly by photons, these types of interactions can be distinguished. This ability is a crucial component to reducing the background of γ-rays, for example, in the search for postulated but not yet discovered particles (35). In addition, NTD Ge thermistors have been used to fabricate the highest-resolution X-ray detectors (36, 37).

Following these discussions about the historical developments of Ge detectors and associated applications, we discuss some technical details in the operation of Ge detectors to explain why Ge detectors are still the gold standard and then illustrate some of the progress achieved.

1.2. Technical Review

Several fundamental physical properties make Ge appealing for the detection of γ radiation. The unique combination of the underlying crystal properties and the unprecedented purity enables γ-ray detection with high efficiency, good signal-to-background ratio, and good timing and excellent energy resolution. **Table 1** summarizes some of the important properties of Ge.

Gamma-ray detection is based on the effect of a γ-ray interacting with matter (38, 39). Three types of interactions are important for γ-ray detection in the range of interest for Ge detectors here, for example, from 10 keV to 20 MeV: the photoelectric absorption, the Compton effect, and the pair production. In Ge, below 150 keV the photoelectrical absorption dominates, between 150 keV and 8 MeV the Compton

Table 1 General properties of Ge

Crystal structure	Lattice constant (Å)	Z	Density ($g\,cm^{-3}$)	Band gap (eV) (77° K)	Pair creation energy (eV) (77° K)	Dielectric constant	ρ at 25°C (Ω cm)	μ_e ($cm^2\,V^{-1}\,s^{-1}$) (77° K)	μ_h ($cm^2\,Vs^{-1}$) (77° K)	τ_e (s)	τ_h (s)	$\mu\tau_e$ ($cm^2\,V^{-1}$)	$\mu\tau_h$ ($cm^2\,V^{-1}$)
Cubic	5.65	32	5.32	0.7	2.96	16	47	3900 (36,000)	1900 (42,000)	$>10^{-3}$	10^{-3}	>1	>1

scattering process, and above 8 MeV the pair production has the largest cross section. Details on these interaction mechanisms can be found in textbooks, for example, the one by Knoll (40). A γ-ray of approximately 1 MeV typically interacts two to three times in a Ge detector via Compton scattering before it is fully absorbed by photoelectric absorption.

In the following we discuss some basic operational aspects in using Ge detectors in ionizing mode. We then discuss some specific characteristics and finally describe pulse shapes obtained and used in segmented Ge detectors.

1.2.1. Basic operation of germanium detectors. The interaction processes briefly described above generate primary charge carriers such as the photoelectrons or Compton electrons through ionization of the Ge atoms. These primary charge carriers generate electron-hole pairs while slowing down. Electrons and holes drift under an external electrical field to the respective electrodes, where they induce a displacement current that can be measured in an external circuit. To measure this current above the leakage current, Ge detectors are operated in reverse-biased diode configuration, which is based on a p-n junction extending from the so-called rectifying contact or electrode. As in a diode, a region can be formed that is depleted of free charge carriers and characterized by very low leakage current. To reduce the otherwise overwhelming leakage current due to the small band gap and associated thermal excitation of intrinsic charge carriers, Ge detectors must be cooled down to below 120 K. Depending on the electrically active net-impurity concentration N in the Ge crystal, the full crystal volume can be depleted by applying a voltage V_d. In a planar detector with thickness d, the depletion voltage can be calculated by

$$V_d = \frac{N d^2}{2\varepsilon},$$

with ε the dielectric constant of Ge. P-type detectors are characterized by acceptors dominating the impurity concentration; in n-type detectors, the donors dominate. The type of crystal produced can be manipulated by doping the material. Two different configurations have been established for Ge detectors: a planar disk and a cylindrical or coaxial geometry.

In a planar configuration, the electrical contacts are provided on the two flat surfaces of the Ge disk. The n+ contact is normally formed by Li evaporation and diffusion into the surface of the wafer. The direct implantation of donor atoms such as phosphorus is difficult owing to a required annealing process to remove crystal damage caused by the implantation process and to make the donor atoms electrically active. In a p-type detector, the n+ contact is typically rectifying, initiating the depletion by applying positive voltage. The contact at the opposite face of the crystal must be a noninjecting or blocking contact for the minority carriers. It may consist of a p+ contact made by boron implantation or a metal-semiconductor surface barrier such as gold that acts as an electrical equivalent. The p+ contact is typically less than 1 μm in thickness, the thickness of the B contact is approximately 0.3 μm, and the n+ Li contact can be as thick as 1 mm owing to the diffusion. The latter thickness must be considered when X rays or low-energetic γ-rays are to be measured. However, this

thick dead layer can serve as a passive shield for α particles or low-energy electrons or photons.

To achieve good charge collection throughout the crystal, voltages significantly higher than the depletion voltages are applied to ensure sufficiently high electrical fields to saturate the drift velocities of electrons and holes and to minimize the collection time and the detrimental effects of charge recombination and trapping. However, the maximum voltage is limited to approximately 5 kV by the leakage currents at the crystal surface and by the additional complexity to prevent high-voltage-induced breakdowns and sparks. Thus, the thickness of the detector is limited to approximately 2 cm in the planar configuration. One challenge in the fabrication of Ge detectors is the passivation of the noncontact surface areas. The goal is to be electrically neutral to establish the wanted field pattern and to withstand high voltages with low reverse-leakage current. One employed technique is to sputter hydrogenated amorphous germanium (a-Ge) onto the etched surface. Despite significant amounts of effort, the passivation of the surfaces is still not electrically neutral and electrical field lines do end on this surface, leading to incomplete charge collection (41). To circumvent the problems associated with these surfaces, so-called guard rings at the edges of the round contacts in planar detectors are introduced that separate the surface effects from the proper bulk properties.

Assuming a low impurity concentration, the electrical fields of planar detectors are almost uniform and holes and electrons drift similarly under the influence of a nearly constant field throughout the active detector volume in p-type and n-type detectors. This is quite different in coaxial detector geometries. Owing to the radial symmetry, electrical fields are nonuniform and the type of the detector has a significant influence on the details of the charge carrier motion. The advantage of the coaxial over the planar geometry is the larger depleted and active volume of a single detector that can be achieved. In addition, the capacitance of coaxial detectors is smaller, resulting in a better signal-to-noise ratio and therefore, in principal, better energy resolution if not for other detrimental effects, for example, charge trapping. While one electrode is fabricated at the outer cylindrical surface of a long Ge crystal, a second cylindrical contact is provided on the surface of an inner borehole. The so-called closed-ended configuration with the borehole reaching through approximately 80% of the detector and the front face as part of the outside contact is preferred over true-coaxial geometries. In this way, only the back side of the crystal must be passivated, with the same complications as the outside edge of planar detectors. In addition, low-energetic photons can enter the active volume, assuming a thin outside contact is being used. The disadvantage of this configuration is a nonuniform electrical field, particularly in the front corners of the detector, which are associated with the weakest electrical fields. To increase the electrical fields in these corners to improve the charge transport, the corners of the crystal as well as the hole are rounded or bulletized. In addition, the higher impurity concentration is chosen for the front of the detector to increase the electrical field as well. In coaxial detectors, the rectifying contact is typically outside to obtain the highest electrical fields outside where most of the detection volume is located. In addition to the thickness of the outside contact, other important criteria in the selection of the type of detector are the susceptibility to

radiation damage and the ability to segment the outer contact. Radiation damage, for example, from neutrons emitted during in-beam nuclear physics experiments or from charged particles in space applications, predominantly generates hole traps. To minimize the hole trapping with its detrimental impact on energy resolution and, ultimately, sensitivity, the hole contribution to the detector signal must be minimized. This can be accomplished by employing n-type detectors to collect the holes outside, with the hole-collecting B-implanted p+ contact outside (42). Another advantage of n-type detectors is the ability to electrically segment the outside B-implanted contact much more easily and reliably than is possible with the thick Li contact on p-type detectors.

1.2.2. Characterization of germanium detectors. Ge detectors are characterized by their excellent energy resolution, good timing characteristic, high efficiency, and peak-to-total ratio. The excellent energy resolution is due to the small energy needed to generate information carriers—in the case of ionization electron-hole pairs—in combination with the high mobility and small charge trapping. As shown in **Table 1**, the mobility-lifetime product $\mu\tau$ is larger than 1, ensuring almost complete charge collection, which is in sharp contrast to all other semiconductor detectors to date except Si. The full width at half maximum (FWHM) of the energy resolution ΔE_{stat} in the statistical limit is defined by the number of information carriers N, which depends on the deposited energy E and the energy required to generate one information carrier ε and the Fano factor F:

$$\Delta E_{stat} = 2.35 \times \sqrt{\varepsilon \times E \times F}.$$

The Fano factor is introduced to reflect the fact that the electron-hole pairs in Ge are not created independently (43). For Ge, it is of the order 0.1. As an example, we assume a γ-ray deposits an energy of 1 MeV in the Ge detector. The average energy to produce one electron-hole pair is 2.96 eV at 80 K (44), and therefore the statistically limited energy resolution is approximately 1.3 keV. The energy to produce an electron-hole pair is approximately four times more than the band gap of 0.7 eV in Ge; that is, $\sim$75% of the energy is converted into thermal energy in the form of phonons. The fact that these two mechanisms are coupled causes the deviation from Poisson statistics and requires the introduction of the Fano factor. In addition to the statistical uncertainty, other factors are limiting the energy resolution, such as carrier trapping and electronic noise. The electronic noise is a function of the leakage current of the detector and the amplification and readout circuitry, which typically consists of a charge-sensitive preamplifier with a field-effect transistor (FET) and a resistive or optoelectronic feedback loop. The noise characteristic of these components, the total capacitance at the FET gate lead to ground—including that of the detector, the leakage current, and any series resistance—and dielectric noise components contribute to the overall electronic noise that can be minimized by adjusting the shaping time in the following processing step. The electronic noise is independent from the energy and typically dominates the resolution at low energies. Details of noise and spectral resolution are described in the paper by Goulding & Landis (45), as well the one by Radeka (46).

Typical energy resolution values for standard Ge detectors are 0.8 keV at 60 keV and 1.8 keV at 1.33 MeV. The low-energy value is dominated by the electronics noise; the higher energy value is dominated by the statistical noise. With small devices, having small-capacity energy resolution values of 110 eV has been achieved at 5.9 keV, with energy thresholds as low as 100 eV (6).

The high purity of Ge detectors is required to deplete all parts of large crystals and provide high fields so that charge carriers can be swept out of the crystal quickly; the low density of shallow traps in combination with the high mobility provide the basis to collect all charges produced owing to the interactions. The mobility-lifetime product in Ge is much larger than the one for holes and electrons in contrast, for example, to the ternary CdZnTe semiconductor that has a mobility lifetime for holes of 10^{-4} (47). Both factors, the high purity and the large $\mu\tau$ product, in addition to the ability to apply high voltages, are necessary for depleting and achieving large volumes of HPGe detectors and therefore high efficiencies.

1.2.3. Signal generation and processing. In this section we briefly review the generation of signals in Ge detectors. The focus here is the dependence and the parameterization of signal shapes with regard to the positions of individual γ-ray interactions. A more detailed description can be found in the review article by Radeka (46).

The motion of charge carriers in the vicinity of an electrode induces a current on this electrode that can be measured. It can be calculated by first determining the path of electrons and holes in the electrical field E_D of the detector, which is obtained by solving the Poisson equation with the proper boundary conditions and the given impurity concentration profile within the detector volume. The path of the charge carrier is calculated by moving the charges through the electrical field with the velocity $v(t)$ given the mobility $\mu_{e,h}$ with $\boldsymbol{v} = \mu_{e,h}\, E_D$. Note that the mobilities in Ge detectors are different for holes (h) and electrons (e) and depend on the temperature and the direction of the motion relative to the crystal orientation (48). In most applications, the original charge cloud extension due to the finite range of the primary electrons such as the Compton electron is neglected, as well as the repulsion and the diffusion of the charges during the charge collection process. However, for detector configurations with segment sizes of the order of millimeters or smaller, the finite size of the charge cloud must be taken into account. Here, charge sharing occurs between segments that can be understood only by taking the underlying processes leading to an extended charge cloud into account. With segment sizes smaller than the charge cloud extension, center-of-charge methods can be applied to improve the lateral position resolution, as discussed by Radeka. These methods are implemented primarily for charged-particle tracking with thin detectors of the order 300 μm and do not require pulse-shape analysis. In applications with thicker detectors and electrode extensions of the order of or slightly larger than the charge cloud extension, this extension must be taken into account if one wishes to achieve a position resolution significantly better than the segment dimensions by pulse-shape analysis. Here, the equations of the electrical field and the motion by diffusion and repulsion must be time dependent and coupled with a finite charge distribution of electrons and holes.

As a second step, the induced current or charge on a specific electrode is deduced by calculating its weighting field. The weighting field is a measure of the electrostatic coupling between the moving charge and the sensing electrode and is calculated by applying a unity voltage to the charge-sensing electrode and zero potential to all other electrodes, with no space charge present. The result is normalized with the voltage to give a dimensionless field. The induced current $i(t)$ in the sensing electrode is then

$$i(t) = -q_m \vec{E}_w \cdot \vec{v}(t),$$

with q_m the charge in motion, E_w the weighting field, and $v(t)$ the velocity of the charge carrier. We can deduce the charge increment $\Delta q(t) = i(t)^* \Delta t$ for every time step Δt and the velocity $v(t) = \Delta r(t)/\Delta t$:

$$\Delta q(t) = -q_m \vec{E}_w \cdot \Delta \vec{r}(t).$$

The true electrical field can be quite different from the weighting field, particularly in segmented detectors. The weighting field is ultimately responsible for the dynamic range of signal shapes that enables a much more accurate position determination than given by the segment size. For example, in the 36-fold segmented prototype detector, which was developed for the Gamma-Ray Energy Tracking Array (GRETA), a position resolution of better than 1 mm at an energy of 374 keV was obtained, which was significantly better than the average segment size of approximately 20 mm (49, 50).

2. RECENT TECHNICAL DEVELOPMENTS

In this section we provide an overview about recent developments in technologies related to the basic performance and operational aspects of Ge detectors. This includes different implementations and configurations such as planar and Ge drift detectors, the encapsulation, amorphous contacts, segmentation schemes, and Ge detectors operated as bolometers. The second part briefly discusses developments in the electronics, including preamplifiers and more recently digital signal processing and pulse-shape analysis. Associated technologies that rely on some of these technologies are finally presented in the third part, such as γ-ray tracking and γ-ray imaging.

2.1. Detector Technologies and Configurations

2.1.1. Encapsulation. To increase the reliability of Ge detectors, the encapsulation technology was developed in the 1990s for nuclear physics experiments (51) and in parallel for space-flight applications (52). A vacuum-tight encapsulation provides several advantages over conventional assemblies: The crystal remains sealed at all times, avoiding contamination of the Ge surfaces, which can happen over time even with small leaks or by annealing the detectors; overall handling is greatly simplified because surfaces are protected; and annealing of radiation-damaged detectors is simplified as well because the capsule can just be put in an ordinary oven. The cold FET is outside the capsule and can be easily repaired or removed before annealing. A defective detector in a multidetector cryostat can be replaced with minimal effort

and without compromising the other detectors. For nuclear physics experiments, the crystal and the capsule have a tapered, hexagonal shape. The distance between crystal surface and can is only 0.7 mm; the thickness of the can is only 0.5 mm. Electron welding of the lid and the electrical feedthroughs at the back ensure a hermetic seal. These features were essential in operating the seven Ge detector cluster detectors for Euroball and the three and four detector modules for Miniball (21). The Miniball detectors demonstrated encapsulation even for two-dimensionally segmented coaxial Ge detectors. Future γ-ray tracking arrays such as GRETA in the United States and the Advanced Gamma-Ray Tracking Array (AGATA) in Europe, consisting of three and four detector modules of (6×6)-fold segmented detectors, will also rely on the encapsulation technology. Without the encapsulation technology, the reliable fabrication, assembly, and operation of these complex detectors would not be possible. Encapsulation for space-based deployment of Ge detectors was developed to address the extreme challenges related to the launch, with extremely high G forces ($\sim$100 G) and the long-term stability with lifetimes of at least five years without any possible human intervention. Although the capsules fabricated for the nuclear physics experiments are kept under vacuum, the capsules for space flights are pressurized to improve the long-term stability. A pressurized can, for example, using ultraclean nitrogen, significantly reduces the inlet of contaminants even in the case of a very small leak and therefore can extend the lifetime of a capsule significantly. It also allows the verification of the proper seal and leak integrity by measuring the nitrogen getting out of the capsule.

2.1.2. Amorphous contact. As discussed above already, Ge detectors—as well as Si detectors as the other elemental semiconductor used for radiation detection—are reverse-biased diodes operated in full depletion, with blocking contacts to maintain low leakage currents and high electrical fields for fast complete charge collection. The contacts on Ge detectors typically consist of n-type contacts formed by Li diffusion and p-type contacts formed by B ion implantation. These contacts are relatively simple to produce and are in use from the beginning of HPGe detector development. However, there are drawbacks in using the Li-diffused contact. This contact produces dead layers typically of the order of hundreds of microns, which prevents low-energy photons from reaching the sensitive detector volume. Thin n-type contacts have been developed using phosphorus implantation; however, they require elaborate processing steps to heal P-implantation-induced defects and cannot withstand high electrical fields (53). Phosphorus-implanted contacts are therefore used only in special applications such as charged-particle transmission detectors. Second, the fabrication of monolithic multi-element detectors using conventional contacts can be difficult because of the need for many processing steps. Finally, the large diffusion depths as well as the high mobility of Li in Ge at room temperature, which increases the size of the contacts, make the formation of small contact structures unreliable (54, 55).

An alternative to these conventional contacts are amorphous semiconductor contacts. The first experimental study of electrical junctions between a-Ge and crystalline Ge was published in 1964 (56). The use of a-Ge to fabricate blocking contacts on Si radiation detectors was first reported in 1971 (57). These contacts showed good

bipolar blocking behavior; that is, they can block both electron and hole injection. A-Ge blocking contacts on HPGe detectors were investigated in 1977, but the devices showed large variations in leakage currents (58). Progress was made by using chemical vapor deposition of amorphous Si on Si detectors (59) and by RF sputtering of a-Ge on Ge detectors (60), instead of using vacuum evaporation deposition. Whereas the first studies used sputtered a-Ge on Ge only on one side to replace either the Li or the B contact, later the bipolar blocking characteristic was used to replace both conventional contacts. Note that the sputtering parameters used originally were identical to those used in the deposition of a-Ge for Ge detector surface passivation (61). Therefore, the a-Ge coating was and still is deposited on the total surface of the Ge. A metal layer, for example, by evaporating aluminum or gold, deposited on the top and the bottom of the detector defines the contact area; the a-Ge on the side and between contact elements serves as a surface-passivation layer. Typical thicknesses for the a-Ge and the metal layers are 300 nm and 50 nm, respectively, and therefore significantly thinner than Li-diffused contacts enabling photon detection down to a few keV that are limited by the entrance window of the cryostat and not by the detector contact. Because the a-Ge represents a true thin dead layer without charge collection, the spectral response for low γ-ray energies is improved over surface-barrier or B-implanted contacts—that is, no significant tails, steps, or generally increased background can be observed. In contrast, surface-barrier or B-implanted contacts generate a partially active layer with low or no electrical field owing to the presence of a high concentration of dopants or defects in which charge loss can take place (62). Even finely segmented contacts are relatively easy to fabricate, avoiding the problem of thick and not temperature-stable Li contacts. Owing to the bipolar blocking character, finely segmented contacts can be made on either side of p-type and n-type detectors, whether in coaxial or in planar configuration. One drawback in operating a-Ge detectors is increased leakage current for increased temperatures, which is due to the reduced barrier heights in these devices as compared with conventional p-n detectors. In addition, temperature cycling between liquid nitrogen and room temperature causes a degradation of the rectifying ability of amorphous contacts. Hull & Pehl (63) recently studied the properties of a-Ge in more detail by producing many detectors and changing sputter parameters such as temperature, time, and sputter gas composition—that is, changing the ratio of H_2/Ar gas concentrations—and found recipes that provide significantly improved performance in terms of temperature cycling and operational temperatures. A-Ge detectors can be operated up to 120 K without significant degradation owing to leakage current, similar to the conventional contacts (64; E.L. Hull, private communication).

2.1.3. Segmentation. The ability to measure the position of γ-ray interactions has many advantages in the detection of γ-rays, for example, for γ-ray tracking and associated γ-ray imaging. Position-sensitive γ-ray detection with Ge detectors was originally realized for nuclear medicine applications by employing arrays of small Ge detectors (65–67). As a more efficient and more practical approach, the segmentation of monolithic Ge detectors was introduced (54, 55, 68, 69). Segmentation of Ge detectors is now normally achieved by segmenting the contacts on the surface of

the detector either by photolithography, simple masking, etching, or even by groove-cutting techniques. Accordingly, they can be more or less invasive, with varying impact on the electrical and charge collection properties in the detector. Segmentation can be implemented as either one-dimensional strips or pixels on one side, or orthogonal strips on both sides. All these implementations have been realized in planar as well as in coaxial Ge detector configurations.

2.1.3.1. Planar high-purity germanium detectors. Segmentation in Ge detectors was first demonstrated in planar HPGe detectors in one-dimensional strip configurations by several groups (54, 55, 69, 70). Photolithography techniques were employed on conventional B-implanted or Li-diffused contacts. To improve the electrical separation of adjacent strips, Protic & Riepe (69) introduced a subsequent plasma-etching process to create grooves of the order of tens of micrometers into the crystal, thereby separating the blocking contacts. With the development of a-Ge contact technologies, the limitations associated with Li-contact segmentation were circumvented and a much less complex segmentation process became possible. Hull & Pehl (63) and Luke et al. (71, 72) use a-Ge sputtering techniques; Protic & Krings (73, 74) use a-Ge evaporation. The contact and segmentation pattern is defined by the evaporation of a metal layer, that is, Au or Al, through a mask. Although Protic et al. use a-Ge contacts only on one side as n+ blocking to replace the Li contact, Luke et al. and Hull et al. coat the total surface with a-Ge, enabling the bipolar blocking characteristics of a-Ge for both contacts and as passivation of the noncontact surfaces. In this way, orthogonal strips on both sides of planar HPGe detectors, so-called double-sided strip detectors (DSSDs), have been fabricated with either n- or p-type Ge material. The ability to use either type of Ge for two-dimensional segmentation in combination with the relative simple processing of a-Ge contacts makes this approach very appealing, in addition to avoiding the limitations of Li contacts such as limited feature sizes >1 mm or long-term stability caused by the high mobility of Li in Ge (55). The a-Ge contact technologies have matured significantly over the past few years and are now available commercially; however, some detrimental effects remain. For example, incomplete charge collection is reported by Amman & Luke (72), which causes a degradation in energy resolution and photopeak efficiency. This specific problem can be avoided by employing field-shaping electrodes in between the charge-sensing electrodes as suggested by Amman, or by electrically separating the electrodes by controlled plasma etching as demonstrated by Protic (73).

Over the past 10 years, many two-dimensionally segmented planar HPGe detectors were fabricated. They range from one-sided strip and one-sided pixilated to DSSDs. **Figure 3** shows one example of a DSSD made of HPGe, with 39 strips on each side with a pitch size of 2 mm. Shown is the detector in its mount, with the readout components and the discrete preamplifiers outside the cryostat. Applications range from atomic and nuclear physics (75–78) to coded-aperture and Compton-scattering-based γ-ray imaging for astrophysics, biomedical research, nuclear medicine, nuclear safeguards, environmental remediation, and homeland security (79–87). In addition, by combining two-dimensional segmentation with the analysis of signal shapes obtained from the segments, the position resolution in all

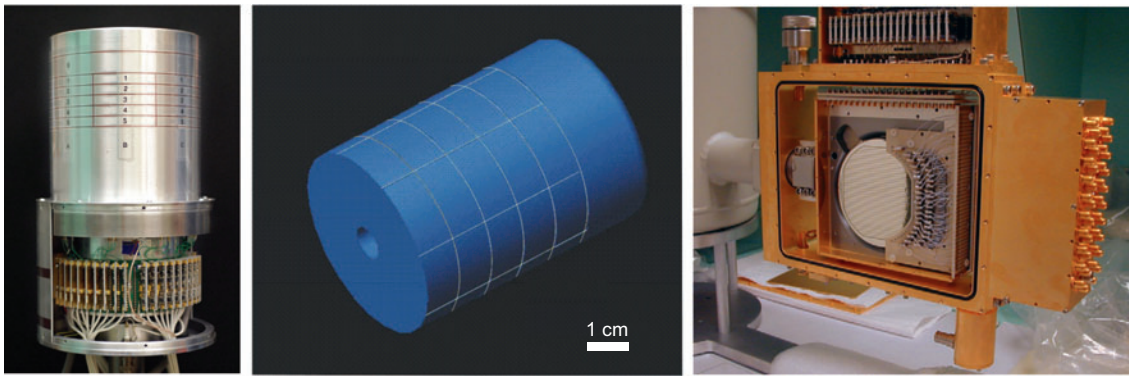

Figure 3

Two types of two-dimensionally segmented HPGe detectors. (*Left and center*) A 40-fold segmented close-ended Ge detector is shown with 5 longitudinal and 8 transversal segments. The 42 preamplifiers to read out the 40 segments, the nonsegmented front cap, and the central channels are arranged on a circular motherboard close to the vacuum feedthroughs. (*Right*) A (2×39)-fold segmented planar detector in double-sided strip configuration is shown. Each strip has a pitch width of 2 mm, resulting in 78 readout channels. As with the coaxial detector on the left, the discrete preamplifiers are operated with warm JFETs mounted close to the vacuum feedthroughs.

three dimensions within the detector can be increased significantly. This aspect is discussed in Signal Processing and Advanced Data Analysis below.

2.1.3.2. Coaxial high-purity geramium detectors. Driven by the demands to increase the sensitivity in nuclear structure experiments, the segmentation of coaxial Ge detectors was pursued from the early 1990s. The first segmented coaxial Ge detectors were fabricated and deployed for the Gammasphere spectrometer (88, 89). The purpose of the twofold segmentation of the outside contact was the increase in position resolution to reduce the impact of Doppler-shifted γ-rays. The Doppler shift of γ-ray energies emitted from excited nuclei in flight can cause a significant degradation in energy resolution owing to the finite size of Ge detectors observing the γ-ray.

Since the end of the 1990s, researchers have pursued three main approaches in segmenting and arranging coaxial HPGe detectors to build arrays of these detectors, providing high photopeak efficiency and excellent (ideally close to the intrinsic) energy resolution for nuclear physics experiments, both owing to the increased granularity provided by segmentation and advanced signal processing. The first and most advanced approach consists of two-dimensionally segmented and individually encapsulated detectors, with several of these detectors arranged in one closely packed cryostat. The aforementioned Miniball array as well as both GRETA in the United States and AGATA in Europe, γ-ray tracking arrays currently being developed, are based on this approach (23, 77, 90). Whereas the Miniball detectors mostly have only six transverse segments, the tracking arrays consist of (6×6)-fold segmented Ge detectors. The second approach consists of so-called Clover detectors, each made of

four square-shaped Ge detectors arranged as a clover in one cryostat (19, 20, 91). In contrast to the Miniball detectors, Clover detectors are not encapsulated. Clover detectors are used either with no segmentation or with one- or two-dimensional segmentation. The most advanced concept for segmented Clover detectors is currently being realized at TRIUMF in Canada for the TIGRESS array. In addition to the fourfold azimuthal segmentation of each detector, a longitudinal segmentation is introduced to increase the position sensitivity in the depth of the detector as well (25). In addition, in TIGRESS, the full potential of pulse-shape analysis in this type of detector is realized (92). The third configuration of segmented coaxial HPGe detectors is the two-dimensional segmentation of HPGe detectors in the original cylindrical shape. One example is an (8×4)-fold segmented detector for the SEGA array currently in operation at the University of Michigan in the United States (24). In the SEGA configuration, the eight longitudinal segments, each 1 cm long, provide the granularity for Doppler-shift correction owing to the alignment of the detector symmetry axis preferentially in parallel to the beam axis. A 40-fold segmented coaxial HPGe detector shown in **Figure 3** was developed by Lawrence Livermore National Laboratory (LLNL) to demonstrate Compton imaging in this type of detector. This detector is segmented in eight azimuthal and five longitudinal segments, the latter covering only the true-coaxial part of the detector to provide maximum position sensitivity, particularly by combining the high segmentation with three-dimensional pulse-shape analysis (93). In Italy, a (6×4)-fold segmented coaxial HPGe detector was fabricated as a part of the European γ-ray tracking effort (94).

Note that all segmented coaxial HPGe detectors are of n-type, with external segmentation of the B-implanted contact. Except for the Gammasphere detectors, all the above mentioned detectors provide the high voltage to the central Li-diffused contact, which requires AC coupling to read out the signal from this side. In Gammasphere, the high voltage was split for the two external segments and the central core was DC coupled. The use of n-type crystals provides (*a*) a reliable and flexible segmentation, (*b*) reduced sensitivity to radiation damage, important for nuclear physics experiments, and (*c*) less attenuation, particularly of low-energy photons in the external contact.

Whereas most of the above mentioned applications aim at nuclear physics and ground-based experiments, one-dimensionally segmented detectors were fabricated for the Reuven Ramaty High-Energy Solar Spectroscopic Imager (RHESSI) space mission to measure X rays and γ-rays from the sun (28). The spectrometer consists of nine HPGe detectors, each with two longitudinal segments. Here the Li-diffused inner contact of the n-type detectors was segmented by cutting a groove approximately 1 cm away from the closed end of the central hole. The purpose of this segmentation was to minimize external space requirements and to separate the smaller front and pseudoplanar part and the back and nearly true-coaxial part of the detector. The front part is used primarily for low photon energies ranging from 3 keV to150 keV, providing excellent timing and energy resolution as well as fast timing characteristics necessary for the occasionally appearing high flux of low-energy photons from the Sun; the back part is used for higher photon energies with significantly reduced photon flux.

Two efforts, one in Liverpool, United Kingdom, and one for Majorana in the United States, evaluated the two-dimensional segmentation of both the external

B contact and the internal Li contact, similarly to the double-sided strip configuration of planar detectors discussed above. These two detectors were fabricated with six azimuthal and external (B-implanted) contacts and two longitudinal and internal (Li-diffused) contacts. In this way, a granularity similar to a 12-fold segmentation can be realized with only eight segments. Initial studies showed degraded performance in energy resolution. Research to characterize and potentially improve the performance of these detectors is still ongoing (A. Boston & A. Young, private communication). Finally, research is also pursued to externally segment p-type detectors by separating the Li-diffused contacts mechanically by precision cutting. By cutting grooves a few millimeters deep and a few millimeters wide, the Li can be separated sufficiently to prevent merging by migration over time. However, the impact of these large grooves remains to be evaluated, particularly with regard to pulse-shape analysis, energy resolution, and efficiency (F. Avignone, private communication).

2.1.3.3. Germanium drift detectors. Luke et al. (95) demonstrated the successful fabrication and operation of a low-capacitance and large-volume Ge detector in 1989. The configuration is similar to the more widely used implementation of Si drift detectors characterized predominantly by electrical fields in parallel to the surface of the detector. In contrast to the Si drift configuration, the Ge-based instrument is aimed at large volumes with a radius of 5 cm or larger and a depth of 5 cm or larger while maintaining the excellent noise performance owing to the small capacitance. In this configuration, the inner hole of a conventional closed-ended coaxial detector is reduced to a small disk 0.5 mm in length and 2 mm in diameter, resulting in a capacitance of approximately 1 pF at full depletion, which is much less than the typical 20 pF observed in conventional coaxial Ge detectors. The Ge drift detector was implemented using n-type material, with the p+ contact outside and the n+ contact inside. In this way, the electrons are the dominant charge carriers producing the detector signal, as almost the full signal is induced as the electrons approach the small n+ contact. The drawback of this configuration is the weak axial electrical field, which causes long electron drift times and associated susceptibility to electron trapping, degrading the energy resolution. To increase the electric field, particularly the axial component, one can either taper the detector, which implies losing a substantial amount of Ge material, or one can use materials with an axial impurity concentration gradient. This gradient is generally intrinsic to Czochralski-grown Ge crystals and more pronounced in n-type crystals owing to the segregation of impurities during the crystal growth process. In the fabricated detector, the impurity concentration was 0.7×10^{10} cm^3 at the closed end and 1.5×10^{10} cm^3 at the small electrode side. Significant electron trapping was observed, leading to an unacceptable energy resolution. By increasing the temperature of the crystal from 77 K to 125 K, the energy resolution was improved to 3.5 keV, with a long shaping time of 32 μs. The improvement of the energy resolution for higher temperatures is attributed to the more rapid release of trapped carriers; the long shaping time helps in collecting the trapped carriers over a longer time period. Although the energy resolution is degraded, the demonstrated noise level was still as low as 270 eV and could be lowered to below 100 eV by employing a better preamplifier such as a pulsed-reset preamplifier and a properly mounted FET. This

noise level is significantly better than the 500 eV that can typically be achieved in coaxial Ge detectors of this size. Very recently, a Ge drift or so-called modified-electrode or point-contact HPGe detector was built in p-type configuration with significantly improved energy resolution (J. Collar, private communication). The low noise and the long drift times can be used to differentiate between single-site and multiple-site interactions in the crystal. This is due to the small pixel effect discussed above, which causes the main charge induction on the small charge-collecting electrode just before the charge carrier reaches the electrode. The low noise and therefore low trigger threshold as well as the ability to distinguish single from multiple interactions with high sensitivity and with only one electrode make it very appealing for experiments aimed at detecting low-energy particles such as WIMPs, low-energy solar neutrinos, or the $0\nu\beta\beta$ decay. The Majorana collaboration is currently considering large-volume Ge drift detectors as detector geometry to search for the $0\nu\beta\beta$ decay.

2.1.3.4. Mechanical cooling. The operating temperature of Ge detectors of approximately 100 K or less is one of its drawbacks, particularly for applications for unattended or remote detection on Earth or in space, where liquid nitrogen as coolant is not readily available. Mechanical cooling is the means to providing sufficient cryogen-free cooling for applications such as space-based missions and nuclear safeguards and customs. Mechanical cooling was originally developed in the 1990s with Joule-Thompson-based coolers with heavy, high-power compressors that could cool, in principle, any size of available Ge detectors. The next step in the development was based on the Kleemenko cycle with mixed gas refrigerants, realized in the commercially available X-COOLER by Ortec (96). Now, typically, Stirling-based cryocoolers are used, which are more efficient, more compact, and require significantly less power. However, one challenge with the Stirling coolers coupled directly to the Ge detector cryostat is the vibration-induced microphonics in the detector readout that degrades the achievable energy resolution in these systems. Complex passive and active compensation schemes or tandem coolers running in antiphase, as well as digital filtering algorithms, have been developed to minimize the impact of microphonics. Whereas the first Stirling cycle system developed by LLNL required approximately 75 W, currently available systems such as the Cryo3 requires only 15 W, weighs approximately 4.5 kg, and can be operated up to 6 hours with one set of batteries (97).

Mechanical cooling for space missions provides not only a reliable way for cooling over long periods of time, it also allows temperature cycling, including necessary annealing of radiation-induced defects, particularly important for long-duration flights such as the Mercury Surface, Space Environment, Geochemistry, and Ranging mission (MESSENGER) (98, 99). Other examples of mechanically cooled Ge detectors are RHESSI in the United States, the International Gamma-Ray Astrophysics Laboratory (INTEGRAL) in Europe, and the Selenological and Engineering Explorer (SELENE) in Japan (100–102). The MESSENGER mission represents one of the most challenging ones and aims at mapping γ-ray emissions from Mercury's surface, for example, to search for ice or water at the poles. Whereas the actual measurements in an orbit of Mercury are expected to take approximately one year, the travel to Mercury alone takes approximately seven years. The MESSENGER spacecraft was

launched in 2004 and is expected to reach Mercury's orbit in 2011. A sophisticated radiation shield and Kevlar suspension were developed to maintain an operational temperature of approximately 85 K despite the extreme temperature changes expected during this mission.

2.2. Electronics

In parallel and closely related to the advances in Ge detector and other radiation detector technologies was the development of the appropriate electronics to optimize the extraction of application-specific features such as energy, time, or position. Only owing to the progress in low-noise and compact electronics was it possible to realize most of the concepts in radiation detection discussed here. The electronics developments range from analog electronics such as low-noise preamplifiers and pulse-shaping amplifiers to digital electronics with fast and high-resolution waveform digitizers and a variety of increasingly powerful digital processing units.

The function of the electronic signal processing is the determination of the energy, time, and position of the γ-ray from the detector pulse. In an analog system, separated pulse-shaping (filter) circuits optimized for energy and time measurements are used to produce pulses for an analog-to-digital converter and a time-to-digital converter. In a digital signal processing unit, the entire pulse shape from the preamplifier is digitized with a waveform digitizer, and the filtering, energy, and time determination are carried out using digital processing. The basic design principle of the filters is the same whether they are implemented in an analog circuit or in digital signal processing. Digital signal processing provides more flexibility, and the possibility of more complex processing, applications-specific analog circuits can still be more compact and less power demanding. One example is the application-specific integrated circuit (ASIC), which is essential for particle physics experiments with hundreds of thousands or even millions of readout channels. However, for high-resolution systems with high intrinsic capacities such as nonsegmented or segmented, large-volume HPGe detectors with capacities of the order 30 pF, discrete and low-noise JFETs in combination with discrete preamplifiers are still state of the art.

2.3. Signal Processing and Advanced Data Analysis

In this section we discuss recent advances in digital signal processing, which, in addition to two-dimensional segmentation, provides the ability to measure energies and three-dimensional positions of individual γ-ray interactions in large-volume Ge detectors. This enables one to track γ-rays with high efficiency, a prerequisite for the new generation of γ-ray spectrometers but also for γ-ray imaging applications, particularly for Compton imaging.

2.3.1. Signal processing in two-dimensional segmented high-purity germanium detectors. Pulse-shape analysis can be implemented in a nonsegmented coaxial detector to determine the radius of γ-ray interactions. Owing to the $1/r$ component in the electrical field, with r indicating the radius and assuming a small impurity

concentration, high electrical fields are obtained close to the inner contact in coaxial detectors associated with a large induced current or a sharp rise in the charge signal. Using these features, either the time of the maximum current or the rise time of the charge signal, one can determine the radius of a γ-ray interaction within the coaxial part and therefore the bulk of the detector. In Gammasphere, the time of the maximum current is implemented (89); a more detailed discussion on the charge signals to deduce the radius can be found in the review by Kroell et al. (103).

Segmenting the detector contacts enables one to obtain complementary position information of the γ-ray interactions and, ultimately, the full reconstruction of energies and three-dimensional positions of even multiple interactions within one or adjacent segments. In arrays with one- or two-dimensional segmentation such as Miniball, Exogam, or in the future TIGRESS, simple feature-extraction concepts similar to the radius determination discussed above are or could be implemented to obtain complementary information about the location of the first interaction. For example, the amplitude of transient-charge signals induced in adjacent azimuthal segments can be used to determine the azimuthal position with a much better accuracy than the segment size itself. The same is true for longitudinal segmentation, which can improve the accuracy of locating the depth of the interaction. However, ultimately the two-dimensional segmentation in addition to processing of the full signals allows us to deduce the energies and three-dimensional positions of even multiple interactions within one detector, enabling the concept of γ-ray tracking with high efficiency and accuracy and allowing us to significantly improve the sensitivity in the detection of γ radiation, for example, in nuclear physics and γ-ray imaging applications.

One approach to deduce the positions and energies of multiple interactions is based on the so-called signal decomposition concept, which aims at decomposing the measured signal shapes into their single-interaction components by using net-charge as well as transient-charge signals. The single-interaction components are calculated following the description from above. The measured signals are then fitted with the calculated signals, where the number of interactions, their energies, and three-dimensional positions are fit parameters. To limit the large dimension of this problem and achieve decomposition times of the order of milliseconds on a single CPU, particularly noting that at least 6–9 segment signals with typically 20–30 samples must be taken into account, the maximum number of interactions allowed is typically two per segment. **Figure 4** illustrates the signal decomposition concept in a DSSD. A γ-ray of 662 keV from a ^{137}Cs source is measured with two interactions in adjacent segments. Using the four strip signals from the top and the four strip signals from the bottom, we can reconstruct the positions and energies of both interactions shown on the left by fitting the measured signals shown on the right. To demonstrate the improvement in resolution, **Figure 5** shows position spectra of measured intensities obtained at an energy of 122 keV of a ^{57}Co source illuminating the DSSD HPGe detector with a 2-mm pitch size through a 12-mm-diameter shadow mask. To perform the full three-dimensional signal decomposition as illustrated in **Figure 4** in this detector with an 11-mm thickness, the finite extension of the charge cloud was taken into account to treat the significant amount of the observed charge sharing correctly. Position-resolution values of better than 0.5 mm in each of the three dimensions was

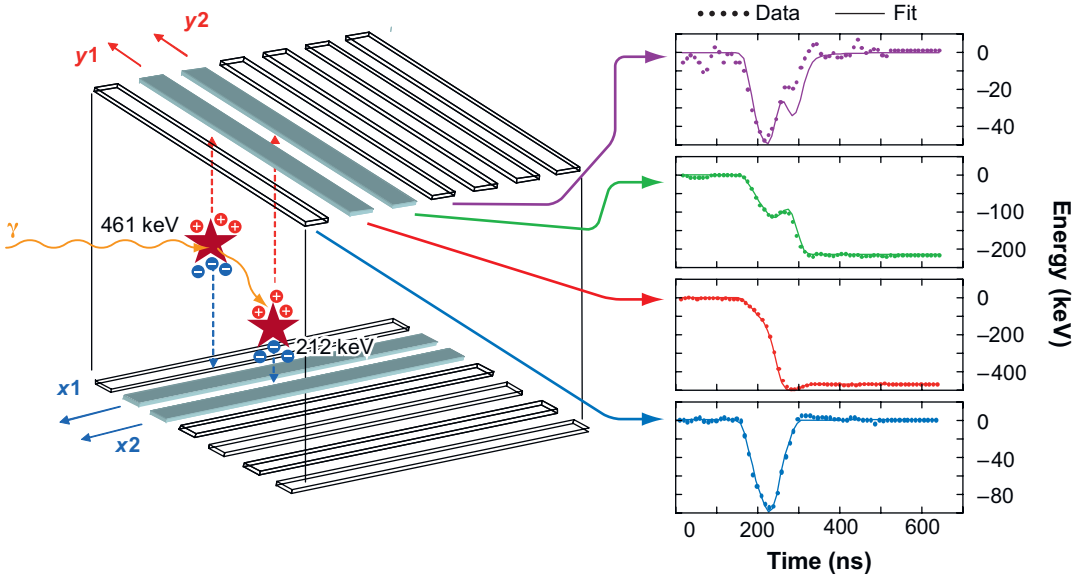

Figure 4

Demonstration of signal decomposition of two interactions in adjacent strips in a double-sided strip detector. By fitting the measured signals of eight strips (only results from the top four strips are shown on the right) with calculated signals, one can determine the energies and three-dimensional positions of individual γ-ray interactions.

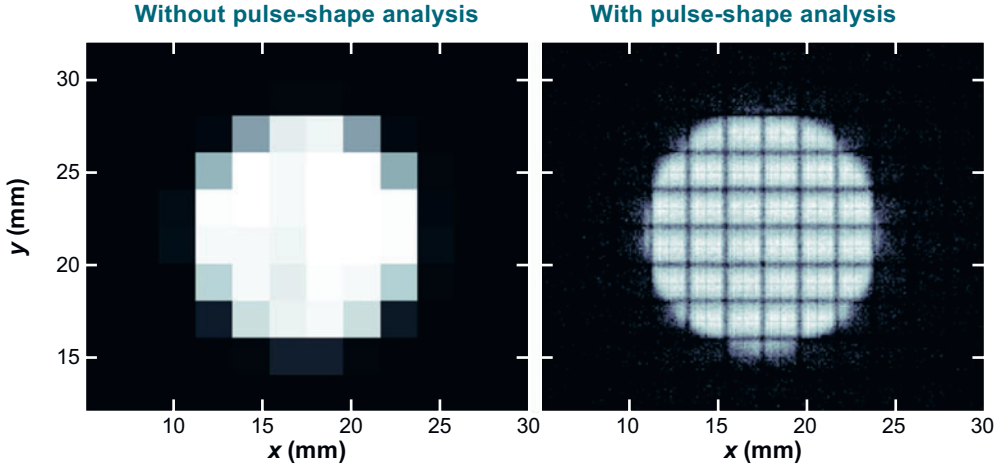

Figure 5

Demonstration of the improvement in the position resolution by applying pulse-shape analysis in a double-sided strip detector. Shown here is a γ-ray shadow of a 12-mm-diameter mask in front of a double-sided strip detector system with a 2-mm pitch size. The left image was obtained without applying pulse-shape analysis, the right image obtained with.

achieved in this detector for energies ranging from 100 keV to 400 keV. The minimum separability, for example, the minimum distance that can be resolved between two interactions, was 1–2 mm. In the GRETA prototype detectors with pixel sizes of the order 2 cm^2, a position resolution of approximately 2 mm was recently demonstrated (I.Y. Lee, private communication).

2.3.2. Gamma-ray tracking. To fully reconstruct or to track the γ-ray in the detector, the γ-ray interactions determined above by signal decomposition or by other means must be time ordered. Owing to the small distance between interactions—a few millimeters to a few centimeters—and a time resolution of typically 5 ns in the Ge detectors, it is not possible to determine the time sequence by measuring the time of the interactions. So-called γ-ray tracking algorithms have been developed, which rely on the characteristics of the underlying physical processes such as Compton scattering, pair production, and photoelectric absorption to order the interactions into a γ-ray path. The focus so far was on Compton scattering and the photoelectric absorption, owing to their dominance in the most interesting region of energies. Several groups have developed γ-ray tracking algorithms for γ-ray spectroscopy and Compton imaging (104–109). They typically determine a tracking figure of merit for all possible permutations of the interactions and use the scattering sequence with the lowest value. However, if the lowest value is above a certain threshold, then it is assumed that the γ-ray escaped the crystal, leaving only a fraction of its energy in the detector. In this way, not only can the scattering sequence of full-energy deposition events be determined, but one can distinguish between full and partial energy deposition and improve the peak-to-total ratio and potentially the overall sensitivity. Owing to the finite accuracy in determining positions and energies of γ-ray interactions, the peak-to-total ratio can be increased, but at the cost of full energy efficiency because some of the γ-rays that deposit their full energy are suppressed too.

These Compton-tracking algorithms typically rely on the Compton scattering kinematics, for example, energy and momentum conservation, the attenuation of γ-rays based on the γ-ray energy and distance to travel between two interactions, and the energy-dependent cross section for photoelectric absorption and Compton scattering. For applications associated with multiple γ-rays emitted and detected simultaneously, as in nuclear physics experiments employing arrays of detectors around a target or a γ-ray source, another so-called clustering algorithm must be applied to distinguish and identify individual γ-rays. As discussed by Schmid et al. (106), the full tracking process for so-called high-multiplicity or high-fold events consists of three parts: the clustering, the tracking, and the recovery. In the clustering step, interaction points within a given angular separation as viewed from the γ-ray source are grouped into a cluster. In the second step, each cluster is evaluated by tracking to determine whether it contains all interaction points belonging to a single γ-ray. Clusters with an acceptable tracking figure of merit are kept; the other clusters are evaluated further in the third step. Here, one tries to recover some of the remaining clusters by adding and subtracting individual interactions or clusters to and from other clusters. Monte Carlo simulations indicate that, given realistic assumptions on position and energy-resolution γ-ray tracking arrays consisting solely of two-dimensionally segmented

coaxial Ge detectors in a closed shell around the target such as GRETA or AGATA, the sensitivity in detection of γ-rays, particularly for high-multiplicity events, can be improved substantially over anti-Compton-based arrays such as Gammasphere.

Gamma-ray tracking not only enables the reconstruction of the scattering sequence and the distinction between partial and full-energy events, it also allows us to reconstruct the full γ-ray energy for some γ-rays that left only their partial energy. Applying the Compton scattering formula, one can calculate the incident γ-ray energy by measuring the energies and positions of at least three interactions (110). Although Wulf (111) successfully demonstrated this method in thin Si detectors in DSSDs, the achievable energy resolution and efficiency are limited by the uncertainties in the energy and positions of the interaction, as well as by the finite tracking efficiency. Although very appealing in Si detectors with its lower Z and density, this concept can also be applied in Ge, particularly for higher γ-ray energies. Knowing the source location, however, allows us to reconstruct the full energy of γ-rays with at least two interactions, owing to the fact that the incident direction is known. This feature points already to the gain from correlating track with image information. How to deduce the image or the location of γ-ray sources is described in the following section.

2.3.3. Compton imaging. The ability to determine the track of a γ-ray in the detector not only allows us to increase the sensitivity for γ-ray spectroscopy, for example, for nuclear physics experiments, but allows us to enable efficient Compton imaging. The concept of Compton imaging, or sometimes known as electronic collimation, was proposed already more than 30 years ago (112, 113). It was realized by the space-based Imaging Compton Telescope (COMPTEL) consisting of two layers of position-sensitive NaI(Tl) detectors and flown in the 1990s. The recent advances in detector segmentation and the development of fast and high-resolution digital electronics allow us now to fabricate Compton-imaging systems built from two-dimensionally segmented Ge detectors, which have significantly higher sensitivity than COMPTEL. **Figure 6** illustrates the concept of Compton imaging. An incident γ-ray interacts at least once via Compton scattering before it is stopped through photoelectric absorption. The energies and positions of these interactions are measured, and through γ-ray tracking the proper scattering sequence is deduced. Employing the Compton scatter formula

$$\cos(\theta) = 1 + \frac{511}{E_\gamma} - \frac{511}{E'_\gamma}; \quad E'_\gamma = E_\gamma - E_1,$$

with θ the scattering angle, E_γ the energy (in keV) of the incident γ-ray, and E_1 the deposited energy in the first γ-ray interaction, the incident direction of the γ-ray can be deduced to a cone with an opening angle θ and a symmetry axis defined by a line connecting the first two interactions. The projection of these cones on a sphere or a plane will overlap at the source location when many events are imaged or back projected. Without measuring the direction of the Compton electron, the incident angle can only be determined to be on a cone surface. Because in Ge the range of electrons is typically below 1 mm (for instance, a 1-MeV γ-ray generates an electron of approximately 500 keV, which has a range of approximately 0.5 mm

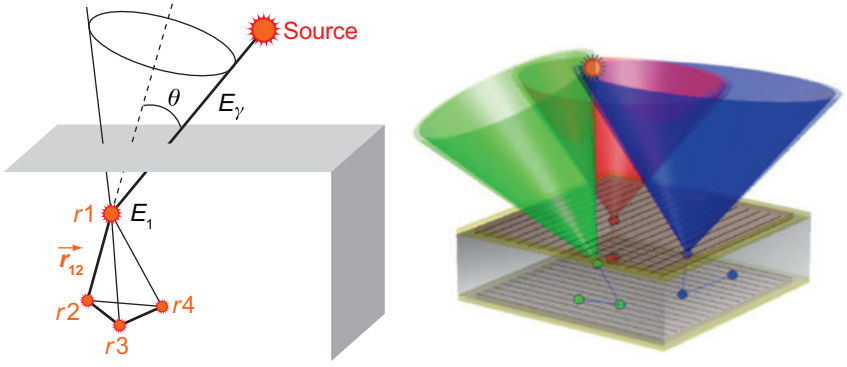

Figure 6

Concept of Compton imaging. With the measurement of individual γ-ray interactions and proper time ordering employing tracking techniques, the positions of the first two interactions as well as the energy of the first interaction can be deduced. Using the Compton scattering formula, it is possible to deduce a cone that defines a surface of possible incident directions for each γ-ray. Because all the cones intersect in the source location, we can form an image by projecting these cones onto a plane.

in Ge), it is very difficult to measure the scattering angle of the electron, particularly considering the complex slowing-down process of electrons. Only in low-Z or low-density detectors, such as gases at a pressure of approximately 1 atm, could electron vertices be measured (114). However, the efficiency to induce a γ-ray interaction at all in these instruments is extremely low. It is interesting to note that Compton imaging has opposing requirements to conventional γ-ray detectors. Although conventional γ-ray detectors aim at high efficiency with high-Z and high-density materials, a Compton imager requires at least one Compton scattering that is well separated from the second interaction to minimize the uncertainty in the direction defined by the first and second interaction for each γ-ray. To induce Compton scattering down to low energies and to maximize the distances between the first interactions, a low-Z and low-density material is required. The position and energy resolution can in principle be improved for better angular resolution, but the electron on which the photon Compton scatters carries momentum, which is inherently unknown and will limit the best angular resolution attainable (115). The most promising approach currently appears to be a hybrid design consisting of Si detectors to meet the requirements for Compton-imaging resolution, and a higher-Z material such as Ge to stop the γ-ray with high efficiency. Ge by itself can also be used as a sensitive Compton imager for γ-ray energies above 500 keV. To improve image quality, a large number of image reconstruction algorithms have been developed (116–119).

2.4. Cryogenic Detectors

The energies of photons and particles are not only lost through ionization, but predominantly by phonon production in detectors. The latter can be measured through an increase in temperatures by making use of the exceptionally small thermal capacity

of materials at low temperatures. Instruments known as bolometers have been used for many years for thermal or infrared radiation in which the incident flux on a target is measured through the temperature rise as sensed by a thermistor. By reducing the temperatures to below 100 mK, it is possible to sense the momentary temperature rise caused by a single photon or incident particle. Although originally Si and Ge were used as absorbers, they are not required as such and other materials can be used as absorbers for γ-rays well. More challenging is the operation of a sensitive thermistor, which can convert the temperature rise into an electric signal as linearly as possible over the full dynamic range of interest. It turns out that NTD detectors made of Ge can meet the necessary requirements. In this way, Ge plays a role either as direct detectors, for example, in searching for cold dark matter (CDM) particles such as WIMPs, or indirectly by providing the thermistor for other materials that are sensitive to either photons or neutrons.

The need for very good energy resolution and the need to detect very small energy depositions in X-ray, γ-ray, or particle detection are the major motivations for the development of low-temperature detectors. Because the energy quanta associated with superconductors and lattice vibrations (phonons) are more than one hundred times smaller, substantial improvements have been obtained in energy resolution and in sensitivity over conventional detectors. Furthermore, these detection schemes permit tailoring of target and absorber materials to match the physics requirements. Examples can be found in particle physics experiments, such as the detection of low-energy neutrinos, search for dark matter particles, search for $0\nu\beta\beta$ decay, and β and γ spectroscopy, as well as X-ray astronomy. Silver et al. (37) report an energy resolution of 3 eV at 6 keV X rays that employ a tin absorber coupled to an NTD Ge thermistor, with a quantum efficiency of approximately 95% at 6 keV. A tin absorber with dimensions of 0.4 mm $\times$ 0.4 mm $\times$ 7 μm was used. Thermalization times, for example, signal rise times of 20 μs, and thermal recovery times, for example, decay times of 250 μs, have been achieved.

3. APPLICATIONS

In this section we discuss four applications of Ge detectors as examples that reflect the benefits of Ge detectors and some of the recent advances discussed before. These examples cover the development of γ-ray tracking arrays for nuclear physics experiments currently under construction in the United States and in Europe; Compton imaging for homeland security and astrophysics applications; the Majorana experiment, which aims at measuring the $0\nu\beta\beta$ decay in ^{76}Ge; and finally the use of Ge detectors to search for WIMPs, as currently being done in the Experience pour Detecter les WIMPs en Site Souterrain (EDELWEISS) experiment and the Cryogenic Dark Matter Search (CDMS) experiment.

3.1. Gamma-Ray Tracking Arrays for Nuclear Physics Applications

Advances in several areas led to the feasibility of large and highly efficient γ-ray tracking arrays: the two-dimensional segmentation of large-volume HPGe detectors, the

pulse-shape analysis to derive energies and positions of individual γ-ray interactions, the tracking algorithms to identify and separate multiple γ-rays and to time order the interactions, the availability of fast and high-resolution waveform digitizers, and finally the availability of sufficient processing power to perform all necessary computations ranging from signal shaping to signal decomposition and γ-ray tracking in real time with event rates up to 50 kHz.

The new generation of γ-ray tracking arrays aims at answering still outstanding questions in the structure of atomic nuclei, particularly nuclei under extreme conditions, thus enabling one to distinguish between theoretical predictions. These instruments allow us to study more complex decay schemes, nuclei at higher spins, larger deformations associated with a large number of simultaneously emitted γ-rays, and collective excitation modes related to high γ-ray energies and their coupling to the normal excitation modes. Finally, these instruments will allow us to discover new excitation modes, as did Gammasphere. In addition, these instruments complement the new generation of radioactive beam facilities that are now either operational, currently being built, or will be built over the next decade. The availability of radioactive nuclei far away from the valley of stability through these facilities coupled with the high sensitivity of γ-ray tracking arrays will enable the study of the structure of nuclei at the boundary of their existence and beyond. Nuclei at extreme spin, isospin, and mass will be explored. The high position resolution and granularity in combination with the high detection efficiency will make γ-ray tracking systems the instrument of choice for both types of radioactive beam facilities, whether Isotope Separator On-Line (ISOL) type or fragmentation type. In addition to nuclear structure studies, other branches of physics will also benefit from the power of γ-ray tracking arrays such as GRETA. For example, the study of the positronium decay into four or five photons would provide higher-order tests of quantum electrodynamics and improve limits on charge conjugation symmetry-violating currents.

Simulations performed for the GRETA array consisting of 120 closed-ended Ge detectors as shown in **Figure 2** predict a full energy efficiency of 50% for a single γ-ray at 1.33 MeV. Assuming a position resolution of 2 mm (rms), which was recently demonstrated with one of the GRETA prototype detectors, the efficiency and peak-to-total ratios are still approximately 25% and 70%, respectively, even if 25 γ-rays are emitted simultaneously. These numbers must be compared with the 8% and 50% obtained for Gammasphere. Because the improvements are per γ-ray, one can understand the increase in overall sensitivity by orders of magnitude, as **Figure 1** illustrates. In addition, the efficiency for high-γ-ray energies is substantially higher, too. At 10 MeV efficiencies, up to 10% are expected, whereas Gammasphere provides only approximately 0.5% at this energy. This gain in efficiency can be explained by the full coverage of Ge detectors, which can contain the larger spatial distribution of higher-energy γ-rays. Finally, owing to the increased number of channels and shorter processing time, one expects to be able to increase the count rate per detector by a factor of five to approximately 50 kHz, reducing the necessary experiment time through larger source strengths or beam intensities, at least for a subset of experiments. The European AGATA effort aims at similar performance numbers. The main differences are the 180 detectors proposed for AGATA, the integration of three instead of four

detectors in one cryostat, and the use of cold FETs inside the cryostat. However, one word of caution is justified here. Previous detector arrays such as Gammasphere relied primarily on simple features defined by the detector and the readout or generally by hardware components only, and therefore the achievable performance was fairly straightforward to predict. In contrast, γ-ray tracking arrays are not only much more complex in terms of the detector and readout hardware, but the overall performance depends strongly on the efficiency and accuracy of the data-processing algorithms, which are much more difficult to predict. Even if all data-processing steps are developed, implemented, and well benchmarked, the variation from detector to detector in terms of crystal dimensions and properties, and in particular variations in the electronic response, for example, impulse response as well as potential cross talk between segments, can not only render the characterization procedures very difficult, but impact the predictability as well. However, even if the simulations overestimate the performance by 10%–20%, the overall gain in introducing these arrays into nuclear physics experiments is substantial and will impact many facets of the atomic nucleus.

Although AGATA and GRETA represent the ultimate goal for nuclear physics experiments, both efforts are currently building smaller arrays. The precursor to AGATA is the AGATA Demonstrator, consisting of five three-detector modules; the precursor to GRETA is termed Gamma-Ray Energy Tracking for In-Beam Applications (GRETINA), consisting of seven four-detector modules. Both are compatible with the larger arrays but allow the demonstration of the overall concept and the expected gain and the initiation of a physics program that makes use of the new capabilities, particularly for the new generation of radioactive beam facilities already in operation or currently being built. For both efforts, the first multidetector module prototype detectors have been fabricated and preliminary test measurements are underway.

3.2. Gamma-Ray Imaging for National Security and Astrophysics

Ge detectors have been developed and are being used for γ-ray imaging applications, either in coded-aperture or in rotation-modulation systems. Examples are coded-aperture imagers with a planar detector in a double-sided strip configuration (120) for nuclear nonproliferation applications, a coded-aperture system combined with an array of 19 nonsegmented coaxial detectors for the space-based γ-ray observatory INTEGRAL, or a rotation-modulation imager consisting of rotating masks in front of an array of seven twofold segmented Ge detectors for the space-based RHESSI program. These imagers use heavy apertures or masks in front of the detector, which increase the weight of the instrument, limit the field of view, and are limited in complex radiation fields owing to the correlation in the data. In particular, for higher γ-ray energies, these systems are limited owing to the need for thicker and hence heavier masks. Furthermore, multiple interactions degrade the imaging performance because the first interaction cannot be determined. The DSSD-based coded-aperture system addresses this problem by placing a large-volume coaxial Ge detector closely behind the planar detector where a γ-ray first interacts in the position-sensitive DSSD and then is fully absorbed in the coaxial detector. Although this approach allows one to

enhance the probability of identifying the first interaction, the main drawback is the loss in efficiency from requiring both detectors to be hit.

The ability to efficiently track γ-rays in three-dimensional position-sensitive detectors allows us to build a new generation of Compton-imaging systems. Because no collimator or space or time modulation is required, the problems associated with these collimators and associated correlations in the data can be circumvented. Many approaches are currently being pursued for Compton-imaging instruments ranging from gas- or liquid-based, time-projection chamber-like implementations (104) to semiconductor detectors. The latter includes pixelated CdZnTe and coaxial HPGe detectors (93, 121), high-purity Si- or Li-drifted Si [Si(Li)] detectors, HPGe or CdTe detectors in DSSD configuration, or a combination of HPSi or Si(Li) with HPGe or CdTe detectors (122–124).

An approach based on HPGe detectors in DSSD configuration is currently being pursued at the Space Science Laboratory in Berkeley as a potential implementation for the next-generation γ-ray observatory—the Advanced Compton Telescope (ACT)—and at LLNL for national security applications. The goal of the ACT mission is to provide unprecedented sensitivity for γ-ray energies ranging from approximately 200 keV to 10 MeV to study several astrophysical phenomena such as supernovae, galactic nucleosynthesis, γ-ray bursts, and fundamental physics (125). The design is driven by its primary science goal, the spectroscopy of the 847-keV transition in ^{56}Co from type Ia supernovae. It will allow the study of hundreds of these events over its five-year survey lifetime, with a sensitivity that is two orders of magnitude higher than that achieved by COMPTEL. Thermonuclear supernovae Ia events are used as standard candles across the Universe to measure cosmological distances and, to a large degree, responsible for the creation of our heavy elements. Yet even those near us are not well understood. The Ge-detector-based Compton-imaging concept as a key component of the instrument was adopted for ACT to maximize background rejection and signal efficiency and to utilize high spectral resolution to dramatically increase the overall sensitivity. In addition, the stringent requirements for size, weight, and power for space-based missions can be met. However, to illustrate the dimension and complexity of the challenge for ACT, an effective area of approximately 1000 cm^2 is required to meet the scientific goals. This goal requires a design for the Ge detector component of only 4 layers of 144 detectors, corresponding to 576 detectors total. Assuming 90×90 strips with a 1-mm strip pitch, approximately 100,000 electronics channels must be read out and processed. Although the lateral positions are deduced by the strips, the depths of interactions are determined by the timing of the opposing electrodes. To meet the performance and the power requirements, new low-noise ASIC technologies that can meet the specific requirements of DSSD HPGe detectors with typical strip and readout capacities of >30 pF are required.

A similar approach based on a combination of three-dimensionally position-sensitive Si and Ge detectors is being pursued at LLNL with the goal of improving the detection of illicit nuclear materials for national security applications such as nuclear nonproliferation and nuclear counterterrorism. Although γ-ray imaging is an established tool in nuclear medicine or astrophysics, only recently has the impact of γ-ray imaging for nuclear security applications been recognized. Here the goal is to

provide improved capabilities to detect, localize, and characterize nuclear materials. One of the outstanding challenges in homeland security is the detection and identification of nuclear threats in a sea of nonthreat objects, which consists of legitimate radioactive objects commonly found in commerce and the environment. To mitigate the primarily nuisance alarms, it is crucial to identify the radioisotope via its characteristic γ-ray decay and to measure the location and the shape of sources through imaging. Gamma-ray imaging can potentially increase the sensitivity in finding such sources, particularly in complex and changing backgrounds owing to the ability to improve signal-to-background ratio. In particular, collimatorless Compton-imaging systems enable one to measure signals and background simultaneously and therefore provide the biggest gain in signal-to-background ratios in γ-ray imaging. Gamma-ray imagers based on position-sensitive semiconductor detectors such as HPGe detectors provide excellent imaging and spectroscopic characteristics and therefore fulfill both important requirements in national security.

At LLNL, a second-generation Compton-imaging system was recently demonstrated, consisting of two large-volume Si(Li) detectors in front of two large-volume HPGe detectors. All detectors are implemented in DSSD configuration with a 2-mm strip pitch. The 10-mm-thick Si(Li) detectors have 32 strips on each side, the 15-mm-thick HPGe detectors 37 strips. The strip signals are read out through external preamplifiers with warm FETs and fed into a digital acquisition system consisting of waveform digitizers operating at 100 MHz with an amplitude resolution of 14 bits. As pointed out above, with this implementation, a position resolution of approximately 0.5 mm in all three dimensions can be achieved. Dividing the total detector volume of approximately 244 ml into $(0.5\ \text{mm})^3$ voxels, we end up with approximately 2×10^6 voxels achieved with only 276 readout channels. This system demonstrated high efficiency, high-energy resolution, and high angular resolution and therefore an overall high γ-ray detection sensitivity for the energies of interest, ranging from 150 keV to approximately 3 MeV. Angular resolution values of approximately 3° at 200 keV and approximately 1° at 1408 keV have been achieved with this approach, and imaging efficiencies between 0.01 and 0.1 are expected for the energy range of interest with the four-detector system.

3.3. Fundamental Physics

Ge detectors have become important tools in fundamental physics studies as well. Two examples are the direct $0\nu\beta\beta$ measurements to infer the Majorana character of neutrinos and to deduce the mass scale of neutrinos and direct WIMP detection. Excellent energy resolution and large sizes of detectors to increase sensitivity in detecting the signal and the deployment deep underground are necessary but not sufficient to suppress the background. Therefore, additional degrees of freedoms to identify and suppress background events have been developed such as pulse-shape analysis and segmentation for Majorana or the correlations between ionization and phonon signals in the WIMP search. The latter rely on the fact that detectors respond differently to electron recoils and nuclear recoils, which can be measured by correlating the ionization with the thermal signal.

3.3.1. Neutrinoless double-beta decay in germanium 76. Recent results from atmospheric, solar, and reactor-based neutrino oscillation experiments have provided compelling evidence that the neutrinos have mass and indicate already that the Standard Model is incomplete. Although the oscillatory character of neutrinos implies that neutrinos have mass, it provides only differences of neutrino masses (e.g., Δm^2). Neutrinoless double-beta decay experiments are the only proposed method of measuring neutrino mass with sufficient sensitivity for masses of interest (below 100 meV) and the only practical method to uncover the Majorana character of the neutrino. The two-neutrino double-beta ($2\nu\beta\beta$) decay is a second-order weak interaction process and has been observed in approximately 10 nuclei (126). The $2\nu\beta\beta$ decay is the transition from the nucleus (A, Z) to the nucleus (A, Z+2) and occurs when the single-beta decay to (A, Z+1) is energetically forbidden, as in most even-even nuclei, or strongly inhibited by a large change of angular momentum. In contrast, in the $0\nu\beta\beta$ decay process, no neutrino is emitted and therefore the process violates lepton number conservation, in contradiction to the Standard Model of particle physics. Whereas the $2\nu\beta\beta$ decay is already a rare process with $T_{1/2} \sim 10^{19}$ years, the $0\nu\beta\beta$ decay is even rarer, with $T_{1/2} > 10^{25}$ years. Because in this process no neutrino is emitted, both electrons always carry the full energy of the Q value. Therefore, the $0\nu\beta\beta$ decay process is characterized by a discrete energy release higher than the energy release of the $2\nu\beta\beta$ decay, which always is the dominating process.

The most sensitive experiments to date are experiments employing Ge detectors in conventional, closed-ended coaxial geometry. In one of the naturally occurring Ge isotopes, ^{76}Ge, the single-beta decay to ^{76}As is energetically forbidden and the $2\nu\beta\beta$ decay to ^{76}Se has been observed. In ^{76}Ge, the $0\nu\beta\beta$ decay is characterized by a discrete energy at 2039 keV. The most sensitive experiments to date have been the Heidelberg-Moscow experiment (127) and the International Germanium Experiment (128), both of which used Ge material enriched to approximately 86% ^{76}Ge, employing centrifuge separation, and both have been completed. Both experiments aimed at extremely low levels of background by using radio-pure materials and active and passive shielding as well as by operating in deep-underground laboratories to reduce cosmic-ray-induced backgrounds. In addition, at the later stages both experiments employed pulse-shape analysis to differentiate between the $0\nu\beta\beta$ process and background events within the Ge detectors. Although the $0\nu\beta\beta$ process is characterized by the emission of two ~1 MeV electrons and therefore a localized energy deposition within approximately 2 mm—reflecting the range of these electrons in Ge—background events at 2039 keV are likely due to γ-rays interacting multiple times throughout the Ge detectors. Employing pulse-shape analysis of the central detector channels, both experiments increased the sensitivity for the $0\nu\beta\beta$ decay significantly by reducing the background rate around 2039 keV to approximately 0.1 events kg^{-1} $year^{-1}$ keV^{-1}.

The Heidelberg-Moscow experiment has two successors, GENIUS (GErmanium in liquid NItrogen Underground Setup) and GERDA (GERmanium Detector Array) (129, 130). GENIUS consists of so-called naked enriched Ge detectors directly in liquid nitrogen. In this way, liquid nitrogen is used not only as a coolant but also as a passive shield and in addition minimizes the amount of background due to potentially contaminated support materials close to the detectors. The GENIUS test facility,

with six naked and natural Ge detectors with a total Ge weight of 15 kg, has been in operation since 2004. Only recently were significant problems in the long-term behavior of this approach identified, which were associated with background from ^{222}Ra diffusing into the setup and, more importantly, an unacceptable increase of leakage current, which renders the detectors almost nonoperational.

GERDA aims at deploying two-dimensionally segmented, enriched ^{76}Ge detectors also immersed in liquid nitrogen or liquid argon. The segmentation of the Ge detectors increases the granularity of the setup over the granularity given by detectors themselves. It also enables pulse-shape analysis of the segment signals and therefore provides complementary granularity to the radius component already available in nonsegmented detectors. The advantage of liquid argon is its higher attenuation of potential background as compared to liquid argon and use as an active shield by detecting the scintillation of background events emitted from either external components or detector components. Currently, (3×6)-fold segmented prototype detectors are being built for GERDA. The Majorana collaboration is currently pursuing research and development, exploring the best approach for a ^{76}Ge-based instrument to observe the $0\nu\beta\beta$ decay based on a staged approach, aiming ultimately at a 1-ton experiment (131). The goal is to demonstrate a background rate of approximately 1 event ton^{-1} yr^{-1} keV^{-1}, which is a factor of 100 below the previous experiments. This will be achieved by reducing external as well Ge detector internal contaminations, employing ultraclean materials that are fabricated underground, and employing advanced technologies such as segmentation and pulse-shape analysis. Preliminary studies with segmented Clover detectors indicate the gain in background suppression by combining segmentation and pulse-shape analysis (132). The fundamental drawback to this approach are the additional components required to read out the additional segments, which contain some degree of radioactive contamination, thereby generating new background. An alternative to segmented detectors represents Ge drift or point-contact configurations. These detectors promise high pulse-shape sensitivity to distinguish multiple interactions with only one readout channel.

3.3.2. Detection of dark matter candidates. In contrast to the $0\nu\beta\beta$ decay discussed above with its single-site discrete energy deposition characteristics at a relatively high energy of 2039 keV, the search for CDM candidates such as WIMPs and the detection of low-energy solar neutrinos are characterized by nondiscrete deposition of energies of approximately 30 keV or less, which is experimentally even more challenging.

In our current understanding of the composition of the Universe, ~70% is contained in dark energy, ~25% can be found as nonbaryonic CDM, and only ~5% can be found as known baryonic matter. WIMPs are the leading candidate for CDM interacting only weakly or not at all with electromagnetic radiation—therefore dark matter. Owing to the mass and velocity of WIMPs relative to the observing detector, the WIMP-nucleus scattering interactions leave recoil energies in the 0–30 keV range. The first generation of experiments in the 1980s with conventional Si and Ge ionization detectors achieved large mass-lifetime exposures and low-background levels owing to underground deployment and the use of low-background

materials. Although from the statistical point of view, these experiments could have been scaled to larger dimensions to achieve significantly higher sensitivity, they are limited by systematic uncertainties owing to the lack of specificity to the nuclear recoil component. Even large-mass systems built of naked Ge ionization detectors will be limited owing to the lack of specificity to background due to both distributed and local contaminations, for example, by uranium or thorium.

With the advent of cryogenic detectors operated at ~20 mK, Ge can be operated simultaneously as a bolometer that measures thermal phonons or a heat and ionization detector when operated as a conventional Ge detector in reverse-biased diode configuration. The amplitude of the phonon signal (measured as an increase in temperature) does not depend on the specific energy loss of either electrons or nuclear recoils. In contrast, in ionization measurements, measured nuclear recoil energies are suppressed or quenched to 25% relative to electron recoils. This difference in response for ionization versus phonon readout can be used to reject electron recoils to better than 99.9% above a threshold of approximately 10 keV. Because the background is due predominantly to X-ray or γ-ray interactions generating electron recoils converted into electro-hole pairs via ionization and the signal—where the scattering of WIMPs on the Ge nucleus is generated by the recoiling nucleus—these two components can be distinguished. Owing to improvements in the readout electronics, the nonthermal phonons can be detected in less than 100 μs. Cryogenic and low-noise detectors provide the necessary signal-to-noise ratio that enables the distinction between nuclear and electron recoils down to low energies, for example, 10 keV, which is critical for detecting WIMPs because the dark matter recoil energy spectrum is exponential and can therefore be confused with electronic noise or other anomalous events.

Examples of experiments using the combined readout in Ge detectors are the EDELWEISS II experiment in the Frejus tunnel, France (133), and the CDMS II experiment in the Soudan mine, United States (134), consisting of 320 g and 250 g of Ge detectors, respectively, both with the goal of deploying 20–30 kg total effective mass and an energy threshold of the order 10 keV. CDMS II also operates Si detectors in the same way to distinguish interactions via spin-dependent and spin-independent coupling.

4. FUTURE DEVELOPMENTS

Developments in Ge detector and related technologies will continue to be driven by the need for new and improved capabilities in the detection of γ-rays and particles. These developments will then enable new ideas and applications in similar or new areas in many different fields. This cycle has been demonstrated with the development of Ge detectors over the past 40 years, and there is no reason why this should not continue.

New technologies are currently being developed, such as Ge drift detectors with the promise of providing excellent energy resolution and sub-keV trigger thresholds in large-volume HPGe detectors. One could envision segmenting the small readout electrode to obtain true three-dimensional information of individual γ-ray interactions. This would be similar to two-dimensionally segmented planar or coaxial Ge

detectors, however, with extremely small capacitance, thus enabling shorter shaping times and, particularly, reduced power requirements, which can be critical for large-scale applications.

The amorphous contact technology has made significant progress, already replacing the Li contact in segmented planar Ge detectors. Only the replacement of the Li n+ contact in DSSDs enabled the recent progress in Compton imaging by providing good energy and position resolutions in addition to high efficiency. In the future it may be possible to grow crystals specifically for planar detectors with just a few centimeters in length but with radii larger than 10 cm, which are currently available and dictated by the production of long coaxial detectors. For comparison, high-purity Si wafers can be grown to 15 cm now and potentially up to 20 cm. However, only up to 2-mm-thick detectors can be made because their purity is lower than that of HPGe detectors. Increasing the detector diameter will allow us to cover larger solid angles and to increase the detection probability without increasing the number of detectors and readout channels as much, effectively reducing the complexity of the instrument and reducing the power requirements. In addition, planar detectors still require guard rings of the order 3–10 mm to separate performance-degrading surface effects from the sensitive detection volume. Developing technologies to reduce or even to eliminate these guard rings will increase the effective detection volume substantially owing to the fact that most of the volume is outside. Reducing the guard ring by 5 mm will typically increase the effective volume by approximately 20%.

Current approaches for Compton imaging and for nuclear physics applications employing planar DSSD systems rely on thick Ge detectors to increase the efficiency. Fast electronics is then required to deduce the depth of interactions, and if the lateral resolution is to be improved beyond the strip size, full digital signal processing is required. Although in this way the efficiency can be maximized with the minimum number of detectors and electronics channels, it is not necessarily the most power-efficient way. Employing thin DSSDs with the resolution defined only by the thickness of the detector and the strip pitch requires slow and less power-consuming electronics to deduce the energy per strip (135). Although a factor of 5–10 more detectors and readout channels are required, the total power requirement can be reduced. In addition, simple multiplexing schemes can be applied to reduce the number of readout channels. In this way, not only can the overall power potentially be reduced, the requirements for impurities and high-voltage can be reduced too, owing to the significantly reduced depletion voltage for thinner detectors.

Over the next five years we will see the first-generation γ-ray tracking arrays, GRETINA and the AGATA Demonstrator, producing the first physics results, very likely at radioactive beam facilities, at least initially. The GERDA effort will have most of the detectors operational underground and looking for the $0\nu\beta\beta$ decay in ^{76}Ge. The Majorana experiment, with the same goal, will have explored a variety of Ge detector configurations suitable for this type of experiment and will likely have demonstrated a specific implementation that can meet the challenging background requirements with a rate of the order 1 count ton^{-1} year^{-1} in the region of interest, which is believed to be necessary for building a 1-ton scale experiment. With regard to space-based missions, MESSENGER will have measured and sent back

the first spectral fingerprints from Mercury's surface. The Ge-based Next Compton Telescope will have explored the feasibility of a large-scale DSSD array for the ACT. For terrestrial applications, more compact and less power-consuming, mechanically cooled Ge detectors will be available for human-operated and remote-detection missions for national security applications worldwide. Arrays of these detectors might even be deployed in specific locations or as surveillance tools. In addition, small arrays of Ge-based Compton-imaging systems will be explored and might be on their way to deployment for homeland security and nuclear safeguard applications.

The recent advances in high-sensitivity, tracking-based γ-ray detection and the availability of fully operational prototypes such as the Si(Li)+HPGe-based Compton-imaging system will allow us to demonstrate the use of these detectors for medical applications as well. Compton cameras can be envisioned as a single-photon emission tomography system for biomedical applications with small animals or for the early detection of breast cancer and improved cancer treatment planning (136). The demonstrated angular resolution in the Si(Li)+HPGe Compton-imaging system, for example, will provide 1–2-mm spatial resolution for γ-ray energies above 300 keV for objects at 10 cm or closer, with sensitivities larger than 10^{-2}. In addition, Compton cameras will provide tomographic imaging without moving the detectors around the object, but only by moving the detection system along one side of the object. Employing large-volume, three-dimensional position-sensitive Ge detectors can also enable one to finally achieve spatial resolution of better than 1 mm for positron emission tomography system, with sensitivities of the order 10%–20% at the same time. Here the challenges are the extremely high count rates due to the amount of radioactivity applied to the patient or the small animal. However, one can estimate that with digital signal processing and adaptive filtering, assuming strip pitches of 2 mm, the count rate capabilities of Ge detectors are sufficient. The energy resolution might be degraded slightly. However, this is not critical to positron emission tomography. Finally, experiments employing the ionization and the phonon mode in Ge aimed at the detection of WIMPs will be fully operational and have collected an unprecedented amount of data, either with a detected signal or with significantly lower limits.

As in the past, the development of Ge detector technologies will be accompanied by advances in electronics and signal processing. They will enable more compact and less power-consuming, low-noise electronics essential for the development of large-scale γ-ray imaging instruments. This will be achieved by advances in analog electronics, with better matched FETs and increased integration, and in digital electronics with lower-power analog-to-digital converters, gate arrays, and processing units with ever more processing capabilities.

Predicting the developments beyond the next five years is inherently more uncertain and speculative, not only owing to the uncertain outcome of the many demonstration experiments and results by the first-generation instruments but also owing to the uncertain overall constraints for basic and applied research and the impact of potentially even more disastrous events than those that have occurred in the recent past. Nevertheless, let us try to speculate assuming basic and applied research continues to be funded as in the past. Assuming the first-generation γ-ray tracking arrays are successful and demonstrate the promised improved capabilities, the full

arrays of GRETA and AGATA will be built and become operational over the next 10 years. At this time, a new generation of radioactive beam facilities above ground but potentially even underground will be available for nuclear physics studies. Gamma-ray tracking arrays will play an essential role in elucidating the structure of the most exotic nuclei at these facilities, but will also provide new insights in phenomena to be explored at stable beam facilities and will be used for complementary fundamental research experiments as well. In parallel, arrays of DSSDs with higher position resolution and imaging capabilities might be operational for specific nuclear physics experiments. The search for the $0\nu\beta\beta$ decay in ^{76}Ge might be underway with a large-scale experiment with hundreds of Ge detectors, might be in Ge drift, might be in two-dimensional segmented configuration, or might even be both combined. Depending on the future vision of NASA, an advanced Compton telescope will be built or under construction, however, not necessarily to the scale envisioned now. Larger-size Ge detector arrays might be deployed either as simple spectroscopy instruments for radioisotope identification or as Compton and coded-aperture γ-ray imaging instruments for search and surveillance applications in homeland security.

5. CONCLUSIONS

Since the introduction of Ge detectors for the detection of γ radiation approximately 40 years ago, the technology has undergone tremendous strides forward in terms of basic and operational capabilities as well as applications. In particular, over the past 10–15 years, the diversity of applications has substantially increased. Ge detectors can now be found on their way to Mercury and looking out even further. Owing to continued improvement and the development of new capabilities in Ge detector and associated technologies, Ge detectors are still playing an essential role in ongoing as well as in future experiments. On the one hand, compact and hand-held Ge detectors are now widely deployed with digital signal processing. On the other hand, large arrays with hundreds of large-volume Ge detectors are operating to look deeper into the structure of the atomic nucleus. The development of two-dimensionally segmented Ge detectors in addition to advances in signal processing enable the concept of γ-ray tracking, with unprecedented sensitivity for nuclear physics applications but also for γ-ray imaging applications, ranging from astrophysics to nuclear medicine to national security. Gamma-ray imaging with Ge detectors can be based on either spatial or temporal modulation systems or aperture- and mask-free Compton imaging. For national security, the deployment of highly efficient and high-resolution detectors is important for nuclear nonproliferation, safeguards, stockpile stewardship, and homeland security, for example, for search and surveillance applications.

Recently the large investment in room-temperature γ-ray detectors led finally to successes, for example, in the fabrication of LaBr scintillation detectors with 2%–3% relative energy resolution at 662 keV and CdZnTe detectors with energy resolution of 1% and better. Although these and other developments to come will certainly at least partially replace Ge detectors, particularly for field applications requiring compact and low-power instruments that can accept degraded energy resolution, Ge detectors will remain the workhorse for many applications for many years to come.

DISCLOSURE STATEMENT

The author is not aware of any biases that might be perceived as affecting the objectivity of this review.

ACKNOWLEDGMENTS

I would like to thank my many colleagues, who I enjoyed working with over the past few years and whose contributions to this review are too numerous to mention. I am particularly grateful to discussions with I-Yang Lee from LBNL, and Dan Chivers, Morgan Burks, and Lucian Mihailescu from LLNL. I am indebted to Paul Luke and Eugene Haller from LBNL for carefully reading this manuscript and for their sensible suggestions. This work was performed under the auspices of the U.S. Department of Energy by LLNL under contract number W-7405-Eng-48.

LITERATURE CITED

1. Tavendale AJ. *Annu. Rev. Nucl. Part. Sci.* 17:73 (1967)
2. Cline D. *Annu. Rev. Nucl. Part. Sci.* 36:637 (1996)
3. Nolan PJ, Twin PJ. *Annu. Rev. Nucl. Part. Sci.* 38:533 (1988)
4. Wu CY, Oertzen WV, Cline D, Guidry MW. *Annu. Rev. Nucl. Part. Sci.* 40:285 (1990)
5. Sangsingkeow P, et al. *Nucl. Instrum. Methods A* 505:203 (2003)
6. Darken LS, Cox CE. In *Semiconductors for Room-Temperature Detector Applications*, ed. TE Schlesinger, RB James, 43:31. Mater. Res. Soc. Symp. Proc. (1995)
7. Elliott SR, Vogel P. *Annu. Rev. Nucl. Part. Sci.* 52:115 (2002)
8. Haller EE, et al. *Proc. 4th Int. Conf. Neutron Transmutat. Doping Semiconduct. Mater.*, ed. RD Larrabee, p. 21. New York: Plenum (1984)
9. Teal GK, Little JB. *Phys. Rev. C* 78:647 (1950)
10. Pell EM. *J. Appl. Phys.* 31:291 (1960)
11. Freck DV, Wakefield J. *Nature* 193:669 (1962)
12. Hall RN, Soltys TJ. *IEEE Trans. Nucl. Sci.* 18:160 (1971)
13. Hall RN. *IEEE Trans. Nucl. Sci.* 21:62 (1974)
14. Hansen WL, Haller EE. In *Nuclear Radiation Detector Materials*, ed. EE Haller, HW Kraner, WA Higinbotham, p. 16. Amsterdam: Elsevier (1983)
15. Gerl J. *Nucl. Instrum. Methods A* 442:12238 (2000)
16. Twin PJ, et al. *Nucl. Phys. A* 409:343 (1983)
17. Deleplanque MA, Diamond RM, eds. *Gammasphere proposal preprint LBNL-5202* (1987)
18. Simpson J, et al. *Z. Phys. A* 358:139 (1997)
19. Azaiez F. *Nucl. Phys. A* 654:1003c (1999)
20. Simpson J, et al. *Acta Phys. Hung.* 11:159 (2001)
21. Eberth J, et al. *Prog. Part. Nucl. Phys.* 38:29 (1997)
22. Habs D, et al. *Prog. Part. Nucl. Phys.* 38:111 (1997)
23. Eberth J, et al. *Prog. Part. Nucl. Phys.* 46:389 (2001)
24. Mueller WF, et al. *Nucl. Instrum. Methods A* 466:492 (2001)

25. Scraggs HC, et al. *Nucl. Instrum. Methods A* 540:348 (2005)
26. Winkler C. *New Astron. Rev.* 48:183 (2004)
27. Ziock KP, et al. *IEEE Trans. Nucl. Sci.* 51:2238 (2004)
28. Lin PR, et al. *Proc. SPIE* 11:3442 (1998)
29. Conka-Nurdan T, et al. *IEEE Trans. Nucl. Sci.* 49:817 (2002)
30. Li H, Clinthorne NH. *IEEE Nucl. Sci. Symp. Rec.* 5:256 (2005)
31. Vetter K. In *Radioanalytical Methods in Interdisciplinary Research*, ed. CA Laue, KL Nash, p. 52. Washington, DC: ACS Symp. Ser. 868 (2003)
32. Vetter K, Burks M, Mihailescu L. *Nucl. Instrum. Methods A* 525:322 (2004)
33. Boggs SE, et al. *Proc. SPIE* 4851:1221 (2002)
34. Kurfess JD, et al. *New Astr. Rev.* 48:293 (2004)
35. Gaitskell RJ. *Annu. Rev. Nucl. Part. Sci.* 54:315 (2004)
36. Alessandrello A, et al. *Phys. Rev. Lett.* 82:513 (1999)
37. Silver E, et al. *Nucl. Instrum. Methods A* 545:683 (2005)
38. Evans R. *The Atomic Nucleus*. New York: McGraw-Hill (1955)
39. Siegbahn K. *Alpha-, Beta-, and Gamma-Ray Spectroscopy*. Amsterdam: North Holland (1965)
40. Knoll GF. *Radiation Detection and Measurement*. New York: Wiley & Sons. 3rd ed. (2000)
41. Hull EL, et al. *Nucl. Instrum. Methods* 385:489 (1997)
42. Pehl RH, et al. *IEEE Trans. Nucl. Sci.* 26:321 (1979)
43. Fano U. *Phys. Rev.* 72:26 (1947)
44. Pehl RG, et al. *Nucl. Instrum. Methods* 59:45 (1968)
45. Goulding FS, Landis DA. *IEEE Trans. Nucl. Sci.* 29:1125 (1982)
46. Radeka V. *IEEE Trans. Nucl. Sci.* 11:358 (1964); Radeka V. *Annu. Rev. Nucl. Part. Sci.* 38:217 (1988)
47. Squillante MR, Shah KS. In *Semiconductors for Room-Temperature Detector Applications*, ed. TE Schlesinger, RB James, 43:465. Mater. Res. Soc. Symp. Proc. (1995)
48. Mihailescu L, et al. *Nucl. Instrum. Methods A* 447:350 (2000)
49. Vetter K, et al. *Nucl. Instrum. Methods* 452:105 (2001)
50. Vetter K, et al. *Nucl. Instrum. Methods* 452:223 (2001)
51. Eberth J, et al. *Nucl. Instrum. Methods A* 369:135 (1996)
52. Cork CP, et al. *IEEE Trans. Nucl. Sci.* 43:1463 (1996)
53. Pehl RH, Luke PN, Friesel DL. *Nucl. Instrum. Methods A* 242:103 (1985)
54. Luke PN. *IEEE Trans. Nucl. Sci.* 31:312 (1984)
55. Gutknecht D. *Nucl. Instrum. Methods A* 288:13 (1990)
56. Grigorovici R, et al. Band structure and electrical conductivity in amorphous germanium. *Proc. 7th Int. Conf. Phys Semiconduct., Paris*, 1964, p. 423 (1964)
57. England JBA, Hammer VW. *Nucl. Instrum. Methods* 96:81 (1971)
58. Hansen WL, Haller EE. *IEEE Trans. Nucl. Sci.* 24:63 (1977)
59. Chiba Y, et al. *Nucl. Instrum. Methods* 299:152 (1990)
60. Luke PN, et al. *IEEE Trans. Nucl. Sci.* 39:590 (1992)
61. Hansen WL, Haller EE. *IEEE Trans. Nucl. Sci.* 27:247 (1980)
62. Luke PN, Rossington CS, Wesela MF. *IEEE Trans. Nucl. Sci.* 41:1074 (1994)

63. Hull EL, Pehl RH. *Nucl. Instrum. Methods A* 538:651 (2005)
64. Pehl RH, Haller EE, Cordi RC. *IEEE Trans. Nucl. Sci.* 20:494 (1973)
65. Detko J. *Phys. Med. Biol.* 14:245 (1969)
66. Schlosser PA, et al. *IEEE Trans. Nucl. Sci.* 21:658 (1974)
67. Kaufman L. *IEEE Trans. Nucl. Sci.* 22:395 (1975)
68. Riepe G, Protic D. *Nucl. Instrum. Methods A* 226:103 (1984)
69. Protic D, Riepe G. *IEEE Trans. Nucl. Sci.* 32:535 (1985)
70. Gerber MS, et al. *IEEE Trans. Nucl. Sci.* 24:182 (1977)
71. Luke PN, et al. *IEEE Trans. Nucl. Sci.* 47:1360 (2000)
72. Amman M, Luke PN. *Nucl. Instrum. Methods A* 452:155 (2000)
73. Protic D, Krings T. *IEEE Trans. Nucl. Sci.* 50:998 (2003)
74. Protic D, Krings T. *IEEE Trans. Nucl. Sci.* 51:1129 (2004)
75. Stoehlker T, et al. *Nucl. Instrum. Methods B* 205:210 (2003)
76. Moore EF, et al. *Nucl. Instrum. Methods A* 505:163 (2003)
77. Deleplanque MA, et al. *Nucl. Instrum. Methods A* 430:292 (1999)
78. Shimoura S. *Nucl. Instrum. Methods A* 525:188 (2004)
79. Ziock KP, et al. *IEEE Trans. Nucl. Sci.* 43:1472 (2004)
80. Inderhees SE, et al. *IEEE Trans. Nucl. Sci.* 43:1467 (1996)
81. Phlips BF, et al. *IEEE Trans. Nucl. Sci.* 43:1472 (1996)
82. Phlips BF, et al. *IEEE Trans. Nucl. Sci.* 49:597 (2002)
83. Yang YF, et al. *IEEE Trans. Nucl. Sci.* 48:656 (2001)
84. Piqueras I, et al. *Nucl. Instrum. Methods A* 525:275 (2004)
85. Vetter K, Burks M, Mihailescu L. *Nucl. Instrum. Methods A* 525:322 (2004)
86. Amrose S, et al. *Nucl. Instrum. Methods A* 505:170 (2003)
87. Boggs SE, et al. *IEEE Trans. Nucl. Sci.* 43:1472 (2002)
88. Lee IY. *Nucl. Phys A* 520:641c (1990)
89. Macchiavelli AO, et al. Performance of Gammasphere split detectors. *Proc. Conf. Phys. Large Gamma-Ray Detect. Arrays Rep.* 35687:149, Lawrence Berkeley Lab., Livermore, Calif. (1994)
90. Bazzacco D. *Nucl. Phys A* 746:248c (2004)
91. De France G. *Eur. Phys. J. A* 20:59 (2003)
92. Svensson CE, et al. *Nucl. Instrum. Methods A* 540:348 (2005)
93. Niedermayr T, et al. *Nucl. Instrum. Methods A* 553:501 (2005)
94. Kroell T, Bazzacco D. *Nucl. Instrum. Methods A* 463:227 (2001)
95. Luke PN, et al. *IEEE Trans. Nucl. Sci.* 36:926 (1989)
96. Lavietes AD, et al. *Nucl. Instrum. Methods A* 422:252 (1999)
97. Becker JA, et al. *Nucl. Instrum. Methods A* 505:167 (2003)
98. Gold RE, et al. *Planet Space Sci.* 49:1482 (2001)
99. Burks M, et al. *IEEE Trans. Nucl. Sci.* 48:656 (2004)
100. Boyle R, et al. *Cryogenics* 39:969 (1999)
101. Wilkinson, et al. *Cryogenics* 39:179 (1999)
102. Kobayashi M, et al. *Nucl. Instrum. Methods A* 548:401 (2005)
103. Kroell T, et al. *Nucl. Instrum. Methods A* 371:489 (1996)
104. Aprile E, Suzuki M. *IEEE Trans. Nucl. Sci.* 36:311 (1989)
105. Dogan N, Wehe DK, Knoll GF. *Nucl. Instrum. Methods A* 299:501 (1990)

106. Schmid GJ, et al. *Nucl. Instrum. Methods A* 430:69 (1999)
107. van der Marel J, Cederwall B. *Nucl. Instrum. Methods A* 437:538 (1999)
108. Lehner CE, He Z, Zhang F. *IEEE Trans. Nucl. Sci.* 51:1618 (2004)
109. Mihailescu, et al. *Nucl. Instrum. Methods A* 570:89 (2007)
110. Kroeger RA, et al. *IEEE Trans. Nucl. Sci.* 49:1887 (2002)
111. Wulf EA. *High resolution Compton imager for detection of shielded SNM*. Presented at Symp. Radiat. Meas. Appl., Ann Arbor (2006)
112. Todd RW, Nightingale JM, Everett DB. *Nature* 251:132 (1974)
113. Schoenfelder V, et al. *Nucl. Instrum. Methods* 107:385 (1973)
114. Bellazzini, et al. *Nucl. Instrum. Methods A* 535:477 (2004)
115. Brusa et al. *Nucl. Instrum. Methods A* 379:167 (1996)
116. Parra LC. *IEEE Trans. Nucl. Sci.* 47:1543 (2000)
117. Shepp LA, Vardi Y. *IEEE Trans. Nucl. Sci.* 1:428 (1982)
118. Wilderman SJ, et al. *IEEE Trans. Nucl. Sci.* 45:957 (1999)
119. Basko R, et al. *Phys. Med. Biol.* 43:887 (1998)
120. Ziock KP, et al. *IEEE Trans. Nucl. Sci.* 49:1737 (2002)
121. Du YF, et al. *Nucl. Instrum. Methods* 457:203 (2001)
122. Bhattacharya D, et al. *New Astr. Rev.* 48:287 (2004)
123. Takahashi T, et al. *New Astr. Rev.* 48:269 (2004)
124. Boggs SE, et al. *New Astr. Rev.* 48:251 (2004)
125. Boggs SE, et al. astro-ph/0608532 (2006)
126. Moe M, Vogel P. *Annu. Rev. Nucl. Part. Sci.* 44:247 (1994)
127. Klapdor-Kleingrothaus HV, et al. *Nucl. Instrum. Methods A* 522:371 (2004)
128. Aalseth CE, et al. *Phys. Rev. D* 65:092007 (2002)
129. Klapdor-Kleingrothaus HV, et al. *Nucl. Instrum. Methods A* 566:472 (2006)
130. Liu X, et al. *Phys. Scr.* 127:46 (2006)
131. Aalseth CE, et al. *Nucl. Phys. B* 138:217 (2005)
132. Elliott SR, et al. *Nucl. Instrum. Methods A* 588:504 (2006)
133. Navick XF, et al. *Nucl. Instrum. Methods A* 559:483 (2006)
134. Mirabolfathi N, et al. *Nucl. Instrum. Methods A* 559:417 (2006)
135. Vetter K, et al. In *Unattended Radiation Sensor Systems for Remote Applications*, ed. JI Trombka, DP Spears, PH Solomon, 632:129. AIP Conf. Proc. (2002)
136. Hartmann-Siantar CL, et al. *Cancer Biother. Radiopharm.* 17:122 (2002)